

Diacylglycerol acyltransferase-1 inhibition enhances intestinal fatty acid oxidation and reduces energy intake in rats^S

Gudrun Schober,^{1,*} Myrtha Arnold,^{*} Susan Birtles,[†] Linda K. Buckett,[†] Gustavo Pacheco-López,[§] Andrew V. Turnbull,[†] Wolfgang Langhans,^{*} and Abdelhak Mansouri^{*}

Physiology and Behavior Laboratory,^{*} Institute of Food, Nutrition, and Health, Swiss Federal Institute of Technology, Zurich, Switzerland; AstraZeneca R&D,[†] Macclesfield, United Kingdom; and Health Science Department,[§] Metropolitan University of Mexico (UAM), Lerma, Mexico;

Abstract AcylCoA:diacylglycerolacyltransferase-1 (DGAT-1) catalyzes the final step in triacylglycerol (TAG) synthesis and is highly expressed in the small intestine. Because DGAT-1 knockout mice are resistant to diet-induced obesity, we investigated the acute effects of intragastric (IG) infusion of a small molecule diacylglycerol acyltransferase-1 inhibitor (DGAT-1i) on eating, circulating fat metabolites, indirect calorimetry, and hepatic and intestinal expression of key fat catabolism enzymes in male rats adapted to an 8 h feeding-16 h deprivation schedule. Also, the DGAT-1i effect on fatty acid oxidation (FAO) was investigated in enterocyte cell culture models. IG DGAT-1i infusions reduced energy intake compared with vehicle in high-fat diet (HFD)-fed rats, but scarcely in chow-fed rats. IG DGAT-1i also blunted the postprandial increase in serum TAG and increased β -hydroxybutyrate levels only in HFD-fed rats, in which it lowered the respiratory quotient and increased intestinal, but not hepatic, protein levels of Complex III of the mitochondrial respiratory chain and of mitochondrial hydroxymethylglutaryl-CoA synthase. Finally, the DGAT-1i enhanced FAO in CaCo2 (EC₅₀ = 0.3494) and HuTu80 (EC₅₀ = 0.00762) cells. Thus, pharmacological DGAT-1 inhibition leads to an increase in intestinal FAO and ketogenesis when dietary fat is available. This may contribute to the observed eating-inhibitory effect.—Schober, G., M. Arnold, S. Birtles, L. K. Buckett, G. Pacheco-López, A. V. Turnbull, W. Langhans, and A. Mansouri. **Diacylglycerol acyltransferase-1 inhibition enhances intestinal fatty acid oxidation and reduces energy intake in rats.** *J. Lipid Res.* 2013. 54: 1369–1384.

Supplementary key words triacylglycerol • ketogenesis • small intestine • enterocytes • high fat diet • eating • acyl CoA:diacylglycerol acyltransferase-1

Obesity is a global epidemic and a major risk factor for type 2 diabetes, hypertension, cardiovascular disease, and other ailments. The development of obesity is multifactorial

This work was supported by Swiss National Science Foundation Grant 31_130665 (W.L.).

Manuscript received 19 December 2012 and in revised form 28 February 2013.

Published, JLR Papers in Press, February 28, 2013

DOI 10.1194/jlr.M035154

Copyright © 2013 by the American Society for Biochemistry and Molecular Biology, Inc.

This article is available online at <http://www.jlr.org>

(1, 2). Often an overconsumption of energy-dense, fat-rich food leads to excessive triacylglycerol (TAG) accumulation in adipose and nonadipose tissue. This can result in insulin resistance and nonalcoholic fatty liver disease, emphasizing the need for pharmacotherapeutic approaches that are effective when a high-fat diet (HFD) is consumed (3).

In the small intestine dietary TAGs are hydrolyzed to 2-monoacylglycerols (MAGs) and fatty acids (FAs) that are absorbed. Specific binding proteins in the enterocytes shuttle MAG and FFA to the endoplasmic reticulum for reesterification. This involves the acylation from MAG to *sn*-1,2-diacylglycerol (DAG) by MAG acyltransferase and the acylation from DAG to TAG catalyzed by acyl CoA:diacylglycerol acyltransferase-1 (DGAT-1) (EC 2.3.1.20), the rate-limiting step in TAG synthesis (4). This MAG pathway is important after eating, when intestinal MAG levels are high (5). DGAT-1 is one of two known DGAT enzymes (6) in tissues associated with TAG synthesis, including the small intestine (6, 7), where DGAT-1 is involved in fat absorption, lipoprotein assembly, and regulation of plasma TAG concentrations (7). DGAT-1 knockout (*dgat-1*^{-/-}) mice are resistant to diet-induced obesity

Abbreviations: AMPK α , AMP-activated protein kinase- α ; ASP, acid soluble products; AUC, area under the curve; BHB, β -hydroxybutyrate; BT, body temperature; BW, body weight; CFA, conditioned flavor avoidance; CPT-1, carnitine palmitoyltransferase-1; DAG, *sn*-1,2-diacylglycerol; DGAT-1, acyl-CoA:diacylglycerol acyltransferase-1; DGAT-1i, diacylglycerol acyltransferase-1 inhibitor; *dgat-1*^{-/-}, DGAT-1 knockout; DIO, diet-induced obesity; EE, energy expenditure; EI, energy intake; FAO, fatty acid oxidation; FCS, fetal calf serum; GLP-1, glucagon-like peptide-1; HFD, high-fat diet; IG, intragastric; JV, jugular vein; MA, mercaptoacetate; MAG, 2-monoacylglycerol; mHMG-CoAS2, mitochondrial hydroxymethylglutaryl-coenzyme A synthase; NEFA, nonesterified fatty acid; PA, physical activity; p-AMPK α , phosphorylated-AMPK α ; PCA, perchloric acid; PVP, polyvinylpyrrolidone; PYY, peptide tyrosine-tyrosine; RQ, respiratory quotient; RT, room temperature; SC, subcutaneously; TAG, triacylglycerol.

¹To whom correspondence should be addressed.

e-mail: gudrun-schober@ethz.ch

^SThe online version of this article (available at <http://www.jlr.org>) contains supplementary data in the form of four figures and six tables.

(DIO) (8), have increased sensitivity to insulin and leptin, decreased TAG levels in liver and skeletal muscle (9, 10), and reduced chylomicronemia after an oral lipid challenge, suggesting reduced intestinal TAG absorption (11). Expression of DGAT-1 only in the intestine of *dgat-1*^{-/-} mice reverses the resistance to DIO and hepatic steatosis, suggesting that the beneficial effects of DGAT-1 inhibition are primarily due to an intestinal action (12). Selectively inhibiting intestinal DGAT-1 might therefore be a promising approach to treat hypertriglyceridemia and obesity (13, 14). Some effects of selective small molecule DGAT-1 inhibitors mimic the features of genetic DGAT-1 deletion, including the prevention of weight gain and the reduction of plasma TAG excursions after oral lipids, but the effects of transgenic deletion and pharmacological inhibition of DGAT-1 on eating appear to be different. Whereas *dgat-1*^{-/-} mice display an increase in food intake, DGAT-1 inhibitors do not stimulate eating (14–16).

We examined the effects of a small molecule DGAT-1 inhibitor (DGAT-1i; Compound 2) (17) on food intake in rats fed HFD or standard chow and started to explore its mechanism of action. To test whether the eating inhibition observed after DGAT-1i administration in HFD-fed rats was related to metabolic effects, we measured circulating metabolites, respiratory quotient (RQ), and energy expenditure (EE) as well as protein expression of hepatic and intestinal enzymes related to lipid catabolism after DGAT-1i administration. In addition, we measured the effect of DGAT-1i on fatty acid oxidation (FAO) in intestinal epithelial cell culture models. A stimulatory effect of DGAT-1 inhibition on enterocyte FAO together with a reduction in food intake would be interesting because peripheral, in particular enterocyte, FAO has been implicated in the control of eating (18).

MATERIALS AND METHODS

Animals and housing

Male Sprague-Dawley rats (6–8 weeks old; Charles River, Sulzfeld, Germany) were housed individually in an air conditioned testing room (22 ± 2°C) with a 12 h light/12 h dark cycle (lights off at 1000 h). During at least 1 week adaptation to housing conditions before catheter implantation (see below) animals were fed ad libitum standard chow or a lard-enriched HFD (60% energy from fat) (Table 1). All experiments were performed in rats adapted to an 8 h feeding/16 h deprivation schedule (food access from 1000 to 1800 h) with continuous access to water unless otherwise indicated. Daily 8 h food intake and body weight (BW) were recorded. All procedures were approved by the Zurich Cantonal Veterinary Office.

Surgery

General. After adaptation to the housing conditions, rats (BW about 300 g) were equipped with chronic intragastric (IG) and jugular vein (JV) catheters as described previously (19) with some modifications (20). The rats had ad libitum access to tap water until 1 h before surgery and they were food deprived for a few hours. Catheters were implanted using sterile techniques. For

infection prophylaxis and analgesia, rats were pretreated with 5 mg/kg trimethoprim/20 mg/kg sulfadoxin (i.e., 200 µl Borgal® 24%; Intervet, Veterinaria AG, Zurich, Switzerland) diluted 1:6 with saline (NaCl 0.9%; B. Braun Medical AG, Sempach, Switzerland) subcutaneously (SC) 3 h prior to anesthesia. Fifteen to 30 min prior to anesthesia, animals were pretreated with 100 µl/100 g atropine SC (0.05 mg/kg/day) (Sintetica S.A., Mendrisio, Switzerland) diluted 1:10 with saline. Inhalation anesthesia was induced with 4–5% isoflurane (Minrad Inc., Provet AG) in oxygen 1,000 ml/min (Pan Gas, Dübendorf, Switzerland). When surgical tolerance was reached, anesthesia was maintained with 1–3% isoflurane, oxygen, and dinitrogenoxide, 300 ml/min each. Eye ointment (Vitamin A 15,000 IE/g; Bausch and Lomb, Steinhausen, Switzerland) was applied, and the animals were kept on heating pads (39°C) throughout the surgery to prevent hypothermia. The depth of anesthesia was checked frequently by testing the interdigital reflexes. One to two hours after surgery and on the following 2 days rats received once daily 100 µl/100 g carprofen (Rimadyl®; Pfizer AG, Zurich, Switzerland) diluted 1:10 with saline (5 mg/kg/day) SC for analgesia and, in addition, trimethoprim/sulfadoxine (5/20 mg/kg) on the day after surgery. During the first week after surgery IG and JV catheters were flushed with sterile saline daily, during the second week every second day, and thereafter every third day. After flushing, all JV catheters were locked with 100 µl sterile heparinized [Heparin-Na (25,000 IU/5 ml); B. Braun] polyvinylpyrrolidone (PVP) solution (PVP-10; Sigma, St. Louis, MO), 21 g PVP/12 ml 0.9% NaCl. All animals were allowed to recover for at least 10 days before experiments began.

Catheter assembly. Both JV and IG catheters consisted of silastic tubing [ID, 0.508 mm; OD, 0.939 mm; length 11.5 cm (JV) and ID, 0.762 mm; OD, 1.651 mm; length 18 cm (IG) respectively; Gore W.L., Newark, DE] with one end slipped on a 20 gauge (JV) or 18 gauge (IG) Vacutainer cannula (Becton-Dickinson, Basel, Switzerland) that was bent into an L shape (>100°) for JV catheters or a U shape for IG catheters. The connection between tubing and cannula was shielded with silicon tubing [ID, 1.016 mm; OD, 2.159 mm; length 1.3 cm (JV) and ID, 1.47 mm; OD, 1.159 mm; length 1.5 cm (IG)] and the proximal ends of both catheters were fixed with 3/0 silk thread (B. Braun, Melsungen, Germany) on a small piece of nonabsorbable polypropylene surgical mesh (2.2 × 3 cm, rounded edges; Bard, NJ). The cannula of the IG catheter protruded cranially from the mesh with a 7–10 mm cranio-caudal distance to the cannula of the JV catheter. In addition, one small JV and three bigger IG bands of silicon (Silicone Adhesive; Cook Veterinary Products, Queensland, Australia) were applied around the tubing at 4 cm (JV) and 0.7, 0.8, and 2.5 cm (IG) respectively, away from the distal end. Two holes were made 0.5 mm away from the distal end of the JV tubing with a 20 gauge needle to reduce adhesion of the catheter to the wall of the atrium during blood aspiration.

Catheter implantation. The cannula ends of the JV and IG catheters were led from a 1.5 cm interscapular incision cranially and exteriorized through a stab wound. The mesh with the cannulas was placed subcutaneously between the scapulae. The distal end of the JV catheter was inserted into the linguofacial vein 2 mm rostral to the bifurcation with the external jugular and maxillary vein and advanced until the silicon band reached the point of perforation. The distal end of the catheter thus lay 2 mm inside the right atrium. The catheter was secured in place by two ligatures, and the cervical skin incision was closed in two layers. Finally, the JV catheter was filled with 100 µl of heparinized PVP solution (see above). The distal end of the IG catheter was then led subcutaneously to a 3 cm midline laparotomy. A small stab wound was made in the wall of the stomach

along the greater curvature, and the catheter was inserted 5 mm into the stomach (until the first silicon band was inside the stomach) and fixed in place with a purse-string suture (4/0 nonabsorbable silk; Johnson and Johnson, Spreitenbach, Switzerland). In addition, the catheter was fixed to the abdominal wall using the third silicon band and nonabsorbable 4/0 silk. The abdominal muscle layer and the skin incision were closed with 3/0 and 5/0 absorbable Vicryl (Ethicon®; Johnson and Johnson) respectively. Small pieces (3–4 cm) of polyethylene tubing [0.76 × 1.22 mm (JV); 1.14 × 1.57 (IG); Smiths Medical, London, UK] were slipped on the cannulas of both catheters and subsequently sealed with a stainless steel pin (“stopper”), which was made out of an obturate blunt 20 gauge needle.

IG catheter verification

IG catheter position and patency was verified post mortem or by X-ray scans [Small Animal Computed Tomography scanner, Zinsser Analytic, La Theta 2.10, Aloka, Tokyo, Japan (settings: slice, multi; number, 10; pitch, 1 mm; speed, fast; position, face down-head front)] (supplementary Fig. 1). For the latter procedure rats were fasted overnight and the X-ray scans were taken under light isoflurane inhalation anesthesia (see above). Diluted contrast agent (1:2; Accupaque TM, GE Healthcare, Chalfont St. Giles, UK; 0.6 ml, 2 parts Accupaque + 1 part saline) was IG infused and scans were taken immediately. Thereafter, the IG catheter was flushed with 0.5 ml saline. All rats recovered from anesthesia within minutes.

Experimental procedures

The DGAT-1i [Compound 2 (17)] was suspended in the vehicle, consisting of 0.5% w/v hydroxypropyl methylcellulose powder (Methocel E4M; Colorcon Limited, Kent, UK) in 0.1% w/v Tween 80 solution (Sigma-Aldrich, Steinheim, Germany) to yield concentrations of 3, 9, or 10 mg DGAT-1i/5 ml vehicle. The suspension was always prepared the day before the experiment and continuously stirred at room temperature (RT) overnight to ensure adequate particle size reduction. The suspension was physically stable for at least 7 days when stored at RT, protected from light, and stirred continuously. IG DGAT-1i or vehicle infusions (5 ml/kg BW; <1 min) were always performed 1 h prior to the 8 h food access beginning at dark onset (1000 h). All rats were adapted to the IG infusion procedure for at least 2 weeks before the experiments.

Energy intake measurements

Cumulative energy intake (EI) was measured manually (± 0.1 g) during the 8 h feeding period (1, 3, 5, 7, and 8 h after food access) after IG vehicle (control) or DGAT-1i (3 and 9 mg/kg BW) administration (1 h before food access) in rats adapted to chow ($n = 4$) or HFD ($n = 5$) (see supplementary Fig. IIA). The effects of the different DGAT-1i doses versus vehicle in both diet groups were tested in two separate within-subjects cross-over trials (1 day between crossovers and 5 days between trials). An additional experiment was performed in another batch of rats adapted to HFD only ($n = 15$) under the same conditions with some modification. In this experiment, EI in vehicle- and DGAT-1i-treated (10 mg/kg) rats was measured electronically every 30 s, as previously described (21), and EI data from defined time points (1, 2, 4, 6, and 8 h after food access) on the experimental day and on the subsequent day without treatment (post-vehicle vs. post-DGAT-1i) were analyzed. The DGAT-1i dose versus vehicle was tested in a within-subjects crossover trial with 1 day between trials.

Conditioned flavor avoidance test

To assess whether rats avoid flavors paired with IG DGAT-1i infusions (10 mg/kg), a two-bottle choice test (22) was performed

in 16 naïve HFD-fed rats. According to a previously described paradigm (23) (with some modifications), rats were adapted for at least 4 days to a drinking schedule with 22.5 h water deprivation and 60 min access to tap water in the morning during the light phase (experimental drinking session; 2–1 h prior to dark onset, i.e., at 0800–0900 h) and 30 min in the afternoon (7.5–8 h after dark onset, i.e., 1730–1800 h); during this afternoon drinking session rats had access to food (see Fig. 2A). During the drinking sessions water was always provided in two bottles simultaneously (e.g., A+B) and the positions of the bottles were switched at mid-fluid access to avoid potential place associations. This drinking regimen was maintained throughout all adaption and experimental stages, and fluid intake was always monitored by weighing the bottles before and after each drinking session. To encourage drinking during short sessions, a 0.2% (w/v) saccharin solution was added to the flavors that were offered during experimental stages (see below). To avoid possible neophobia to saccharin, rats were adapted to the saccharin solution for 2 days. On association days (trials 1 and 2), rats had access to two different flavored solutions [i.e., grape or cherry flavor (0.05% w/v) in 0.2% saccharin solution, unsweetened powdered Kool-Aid drink mix; Kraft Foods, White Plains, NY] during the experimental drinking session in the morning. Shortly after this drinking session, rats were IG infused with either vehicle or DGAT-1i (10 mg/kg BW) 1 h before dark onset (i.e., 0900 h). Both flavors were counterbalanced with respect to drug order and with respect to flavor/drug combinations across the two association days separated by one intervening day (e.g., grape/cherry paired with DGAT-1i (CS+)/vehicle (CS-) on association trial 1, cherry/grape paired with DGAT-1i/vehicle on association trial 2. Two days after the second association trial, a two-bottle choice test was performed in which rats had simultaneous access to both flavors during the experimental drinking session in the morning. The locations (right vs. left) of the two flavored bottles were similarly counterbalanced and bottle positions were switched at mid-fluid access. No IG vehicle or DGAT-1i infusions were performed on this test day and rats were then returned to ad libitum water access. For each rat the percentage of fluid intake from the DGAT-1i-paired flavor (CS+) was calculated using the following equation: CS+ preference (%) = $[V_{CS+} / (V_{CS+} + V_{CS-})] \times 100$, where V_{CS+} is the volume of DGAT-1i-paired flavor intake, and V_{CS-} is the volume of vehicle-paired flavor intake. Vehicle and DGAT-1i flavor preference ratios (CS- preference%:CS+ preference%) from each rat were averaged and a paired *t*-test was used to determine whether differences in preference for vehicle-paired versus DGAT-1i-paired flavors during the choice test were statistically significant. A preference ratio of 50%:50% was considered equal for both flavors (no effect of flavor pairing on intake). A shift in the ratio toward

TABLE 1. Diet content of the regular chow and the lard enriched high fat diet

Major Nutrients	Regular Chow Diet, No. 3433 ^a	High Fat Diet (60% kcal % fat), No. 2127 ^a
Dry matter (%)	88.0	92.0
Crude protein (%)	18.5	23.9
Crude fat (%)	4.5	35.0
Crude fiber (%)	4.5	4.9
NFE (%)	54.2	23.2
Starch (%)	35	1
Crude ash (%)	6.3	5.0
Gross energy (MJ/kg)	16.1	23.8
Metabolizable energy (MJ/kg)	13.2	22.0

NFE, nitrogen-free extract.

^aDiets purchased from Provimi Kliba Nafag, Kaiseraugst, Switzerland.

the vehicle-paired flavor (e.g., 75%:25%) was interpreted as evidence for conditioned flavor avoidance (CFA) (24).

Blood lipid analyses

The effect of acute IG DGAT-1i infusions (9 mg/kg) on serum and plasma fat metabolites was tested in rats that were refed with a 3 g HFD or 5 g isocaloric chow test meal at dark onset after 16 h of food deprivation. All rats were well adapted to this procedure, and the size of the test meal was chosen based on preliminary trials showing that under these conditions all rats finished 5 g chow within 10 min. The experiment was designed as a within-subjects crossover test in each diet group with the treatments given in random order and with 2 days between trials. Blood samples (400 μ l each) were taken via the JV catheter in the fasted state shortly before IG infusions at about 0900 h (baseline) and at 2 (1100 h), 3 (1200 h), and 5 h (1400 h) after IG infusions (see supplementary Fig. IIB). Blood (250 μ l) was transferred into 0.6 ml Eppendorf tubes containing 9 μ l EDTA solution (Titriplex 3, Merck, Germany; 180 mg dissolved in 3.0 ml distilled water), mixed gently, put on wet ice, and centrifuged (10 min, 10,000 rpm, 4°C) within 20 min. The plasma was transferred into Cobas-Mira analyzer cups (Hoffmann La Roche, Basel, Switzerland) and stored at -20°C until analysis (see below). The remaining 150 μ l of blood were transferred into a glass tube (Schmidlin Labor and Service AG, Neuheim, Switzerland) and allowed to clot for 4–5 h at RT. The serum was transferred into Cobas-Mira analyzer cups and stored at 4°C until analysis (see below) later on the same day. Fasting and postprandial serum TAG, plasma free glycerol, nonesterified fatty acid (NEFA), and β -hydroxybutyrate (BHB) concentrations were measured using standard colorimetric and enzymatic methods adapted for the Cobas MIRA® autoanalyzer (Hoffman LaRoche) (25).

Fecal lipid analysis

After an IG DGAT-1i (10 mg/kg) or vehicle infusion (1 h before food access) the feces of 18 rats (n = 9/group) fed a HFD were collected every 2 h during the 8 h food access period in the dark phase and 12 and 24 h after food access during the light phase (see supplementary Fig. IIC). The feces were dried overnight, ground, and fecal fat was extracted via the Folch extraction method (26). The extracted lipids were then dissolved in chloroform:methanol (2:1) and separated by thin-layer chromatography (TLC Silica Gel 60 F254 Aluminum sheets, 20 \times 20 cm; Merck, Germany) using petrol ether (boiling point 40–60°C):diethyl ether:acetic acid (84.5:15:0.5) as migration solvent. After the separation, the silica gel plate was taken out of the hermetically closed glass chamber to dry it and to let the solvent mixture evaporate. The different lipid fractions were visualized using iodine vapor, which colors them brownish/yellowish. Sunflower oil

(100 mg in 10 μ l chloroform/methanol (2:1)/mg) was used as reference (see Fig. 4B). The silica gel plate was cut to collect the NEFA fractions for each animal by scratching off the silica gel of the single pieces. Subsequently, the NEFAs contained in the scratched silica were reextracted with acetone and quantified with an enzymatic colorimetric diagnostic kit (NEFA-HR(2) R1 + R2 Set; Wako Chemicals GmbH).

Indirect calorimetry measurements

Indirect calorimetry was performed in 16 Plexiglas airtight metabolic cages (42 \times 42 \times 30 cm) in an open-circuit indirect calorimetry system (AccuScan Instruments Inc., Columbus, OH) as previously described (with modifications) (27). In a within-subjects crossover design (DGAT-1i vs. vehicle) with two intervening days between trials, rats were single housed on a layer of wood shavings under the same light, temperature, and food access conditions as described above, except that powdered HFD (No. 2127; Provimi Kliba AG) was used to allow for the detection of small changes in food intake. Water bottles and food cups were mounted on electronic balances, and cumulative food and water intakes were continuously recorded in 5 min intervals during the 8 h feeding period. Gas exchange (to calculate EE and RQ) was measured from 1 h before until 23 h after IG DGAT-1i (10 mg/kg) or vehicle infusions given 1 h before dark onset. To measure EE and RQ, ambient air was pumped into the cage via an adjustable flow controller (flow rate set to 1.7 l/min), and O₂ and CO₂ concentrations were measured by two analyzers (for 30 s in 5 min intervals) connected to each cage. This allowed for calculating EE and RQ using the manufacturer's software (PhysioPlot Version 1.80, IntegraME Version 2.21; AccuScan Instruments Inc.). EE was calculated according to Weir (28) using the following equation: total energy expenditure (kcal/kg/h) = [3.9 \times V(O₂) + 1.1 \times V(CO₂)]/1,000; V(O₂) and V(CO₂) were normalized for body weight. The RQ was defined as the quotient of CO₂ production and O₂ consumption.

Body temperature and activity measurements

Body temperature (BT) and physical activity (PA) were measured simultaneously during 1 h before and 23 h after IG DGAT-1i (10 mg/kg) and vehicle infusions throughout indirect calorimetry measurements. DSI PhysioTel® TA-F40 small animal transmitters (Data Sciences International, St. Paul, MN) were implanted into the peritoneal cavity of each animal for body temperature and activity measurements as previously described by Riediger et al. (27). Receiver plates, which were placed underneath the metabolic cages, saved data every 5 min and readouts were then evaluated on a connected computer with the manufacturer's software (Acquisition Version 4.00, Analysis Version 4.00; Dataquest A.R.T.™). The activity data represent an arbitrary unit reflecting

TABLE 2. Antibodies used in Western blotting

Antibody	Molecular Weight (kDa)	Dilution	Vendor	Catalog/Clone Number
Anti-mouse IgG, HRP-linked		1:2000	Cell Signaling Technology	7076
Anti-rabbit IgG, HRP-linked		1:2000	Cell Signaling Technology	7074
Mouse monoclonal anti- β -actin	42	1:3000	Sigma-Aldrich	clone AC-74
Mouse monoclonal anti- γ -Tubulin	48	1:6000	Sigma-Aldrich	T6557/clone GTU-88
CPT-1A	88	1:5000	Gift from C. Prip-Buus ^a	
Rabbit AMPK α	62	1:1000	Cell Signaling Technology	2532
Phospho-AMPK α (Thr172) rabbit mAb	62	1:1000	Cell Signaling Technology	2535
Rabbit anti-HMG-CoA synthase (mitochondrial)	56	1:200	Aviva System Biology	ARP41562_T100
MitoProfile® Total OXPHOS Rodent Ab Cocktail	20,30,40,48,55	1:250	Abcam	Ab110413

^aInstitute Cochin, Département d'Endocrinologie, Métabolisme et Cancer, Paris, France.

locomotor activity and do not relate to an absolute measurement of distance moved.

Analyses of metabolic enzymes in liver and small intestinal mucosa

Tissue sampling and processing. Rats received IG DGAT-1i (9 mg/kg) or vehicle infusions 1 h before dark onset and were refed at dark onset with either a 3 g HFD or an isocaloric 5 g chow test meal, respectively. Rats were then killed by decapitation 2 h after IG infusions and the liver was removed and immediately frozen in liquid nitrogen. The whole small intestine was removed and two segments representing the duodenum (the proximal 20 cm small intestine distal to the pylorus) and jejunum (35 cm) were dissected. The intestinal lumina were gently flushed with ice-cold PBS and the mucosa was carefully scraped off with a glass slide into cryotubes (Nunc Cryotube 1.8 ml) and placed in liquid nitrogen. Liver and small intestine samples were stored at -80°C until further processing. For protein extraction, liver and small intestinal mucosa samples were homogenized in lysis buffer (1% Triton X-100, 100 mM Tris pH 7.4, 400 mM NaCl, 10 mM EDTA) including protease inhibitors (complete, EDTA-free

Protease Inhibitor Cocktail Tablets, Roche). After centrifugation (10 min, 4°C , 16,110 g) the supernatant was removed, and protein concentrations were measured with the Bio-Rad protein assay (BioRad DC Protein Assay; München, Germany), based on the Bradford dye-binding method (29) with BSA as a standard as indicated by the supplier.

Western blotting analysis. Western blotting of carnitine palmitoyltransferase-1 (CPT-1), AMP-activated protein kinase- α (AMPK α) and phosphorylated-AMPK α (p-AMPK α), mitochondrial hydroxymethylglutaryl-CoA synthase (mHMG-CoAS2), and Complex III of the mitochondrial respiratory chain was conducted using standard techniques; antibodies and dilutions are listed in **Table 2**. Briefly, proteins in Laemmli (6 \times) sample buffer (10–30 μg per depot) were separated by 10% SDS-PAGE with either 7 or 12% polyacrylamide for the separating gels. For molecular protein weight estimation, a 3-color protein molecular weight standard was used following the manufacturer's suggestion (PageRulerTM Prestained Protein Ladder; Fermentas). After SDS-PAGE, gels were transferred electrophoretically onto nitrocellulose membranes (pore size 0.2 μm ; Protran, Whatman) and

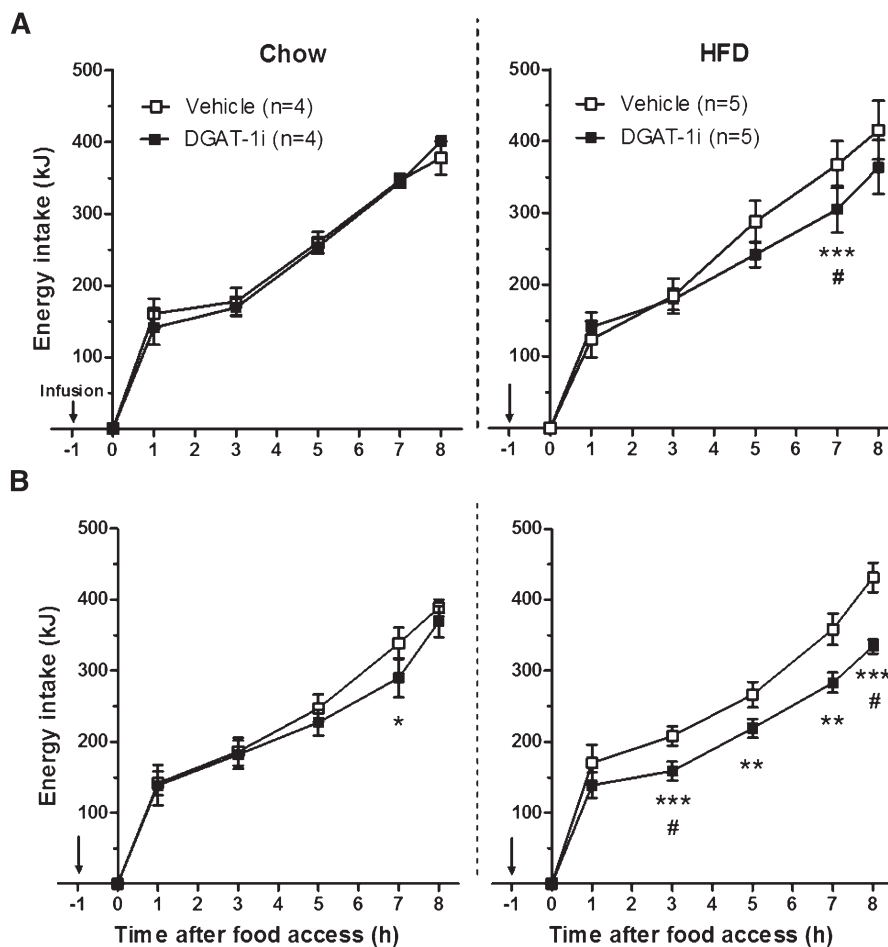


Fig. 1. Acute IG DGAT-1i infusions reduced energy intake mainly in HFD-fed rats. Rats were adapted to chow ($n = 4$) or HFD ($n = 5$) and to an 8 h feeding/16 h deprivation schedule. Acute IG infusions (1; 5 ml/kg) of 3 mg/kg (A) and 9 mg/kg (B) DGAT-1i or vehicle were given 1 h before food access at dark onset (1000 h) and cumulative energy intake was measured during the 8 h feeding period. Data are presented as means \pm SEM and were analyzed for individual time points by a 2×2 mixed ANOVA with diet (chow and HFD) as between-subject and treatment (vehicle and DGAT-1i) as within-subject factors. Significant differences were followed up by Bonferroni-Holm post hoc comparisons. * $P < 0.05$, ** $P < 0.01$, *** $P < 0.001$ versus vehicle, #Significant treatment \times diet interaction ($P < 0.05$).

gel loading was assessed by reversible Ponceau S staining right after transfer. Membranes were rinsed in distilled water until the staining was completely eliminated and subsequently blocked in 5% skim milk in Tris-buffered saline containing 0.1% Tween-20 for 1 h before immunodetection processing. The membranes were incubated with the primary antibodies overnight at 4°C, washed 3 times with Tween-20, and incubated with secondary horseradish peroxidase-conjugated anti-rabbit or anti-mouse IgG, respectively, for 1 h at RT. Protein bands were visualized using a chemiluminescent substrate [1 ml solution A (50 mg luminol in 200 ml 0.1 M Tris, pH 8.6) + 100 µl solution B (22 mg p-coumaric acid in 50 ml DMSO) + 1 µl H₂O₂] and the intensities of the bands were quantified by densitometry using Image J software (ImageJ 1.46b). All Western blots were performed at least 2 times.

In vitro experiments

Cell culture. HuTu80 cells (human duodenal carcinoma cell line, American Type Culture Collection) were maintained in MEM containing L-glutamine plus 10% fetal calf serum (FCS) and 1% nonessential fatty acids (FAs). CaCo2 cells (human

colonic cell line, European Collection of Animal Cell Culture) were maintained in low glucose DMEM supplemented with L-glutamine, penicillin, and streptomycin plus 10% FCS. Confluent layers of CaCo2 cells were maintained up to 25 days in this medium for differentiation.

FAO measurement. FAO studies were performed on confluent layers of cells in 6-well multiwell plates (Nunc, UK) and assessed by the uptake of ¹⁴C-palmitic acid or ¹⁴C-oleic acid and release of ¹⁴C-CO₂ and ¹⁴C-acid soluble products (ASP). For the experiment, the medium was removed and the cells were preincubated for 30 min with 1 ml of the respective medium without FCS containing various concentrations of DGAT-1i (0.1 nM–10 µM) dissolved in DMSO (0.1% final concentration). Control wells received 0.1% DMSO without DGAT-1i. ¹⁴C-palmitic acid (NET043001MC; PerkinElmer, Boston, MA) or ¹⁴C-oleic acid (NET289001MC; Perkin Elmer) (0.12 mM, 1 mCi/well) complexed to essentially fatty acid free BSA (molar ratio 4:1; Sigma, UK) was added to each well for another 2 h incubation at 37°C. To measure FAO by CO₂ release, 900 µl of cell medium from each well was removed to a 7 ml bijou (Sterilin, UK) and 100 µl ice-cold 30% perchloric acid (PCA) was added. The lid containing

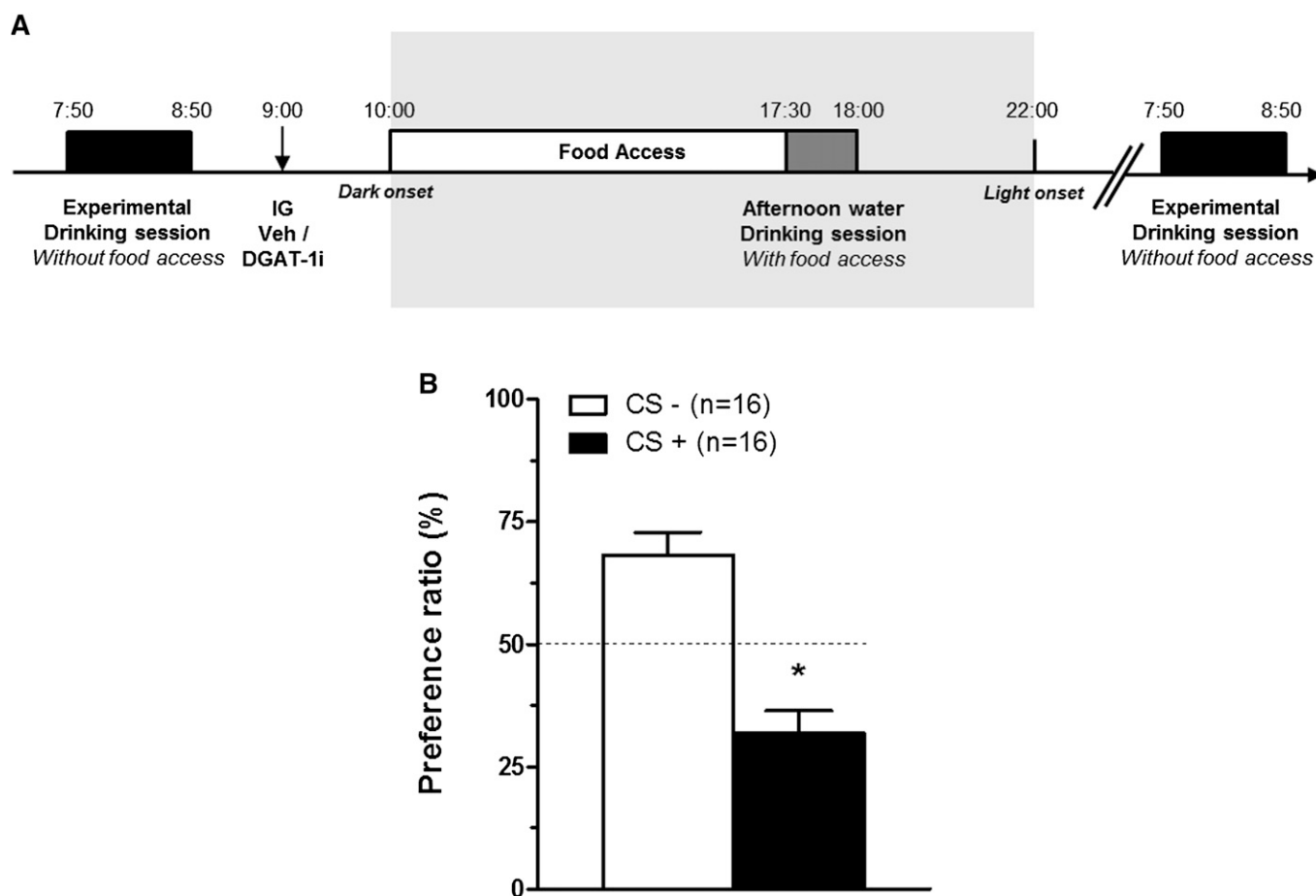


Fig. 2. Acute IG DGAT-1i infusions caused a mild CFA in HFD-fed rats. **A:** Timeline of the CFA paradigm. On the two association days (trials 1 and 2), rats had access to two different flavored solutions (e.g., grape flavor on trial 1, cherry flavor on trial 2, or contrariwise) during the morning experimental drinking session (60 min) (2–1 h prior to dark onset). Immediately thereafter (1 h prior dark onset), rats received either vehicle or DGAT-1i (10 mg/kg) infusions (↓; within-subject design). On the experimental day, a two-bottle choice test was performed during the experimental drinking session in which rats had simultaneous access to the flavor paired with vehicle (CS–) and the flavor paired with DGAT-1i (CS+). **B:** IG DGAT-1i infusion (10 mg/kg) 1 h before dark onset (1000 h) reduced flavor preference in a two-bottle choice test in HFD-fed rats adapted to the drinking schedule described above. The dashed line indicates equal preference for both flavors. Preference ratios (%) are means ± SEM. **P* < 0.05 versus CS– (paired *t*-test).

a filter paper (grade 1 circles, 20 mm diameter; Whatman Schleicher Schuell, UK) impregnated with 100 μ l 0.1 M NaOH was immediately screwed on and the tubes were gently shaken and then left overnight at RT. The filter papers were removed and placed in scintillation vials. Four milliliters of scintillation fluid were added and CO₂ production was counted. To measure FAO by PCA for ASP, the remaining medium was transferred to Eppendorf tubes, centrifuged (16,500 g, 5 min, RT), and 800 μ l of the supernatant was transferred to scintillation vials and counted. The effect was calculated by adding the counts (CO₂ production) on the filter paper to the counts in the supernatant (ASP).

Statistical analysis

Statistical analyses were performed using the SPSS software package (SPSS Inc., version 19.0, Chicago, IL) or GraphPad Prisma (GraphPad Software, version 5.00 for Windows, San Diego, CA). ANOVA assumption of data homogeneity and normality and repeated measures-ANOVA assumption of sphericity were checked and, if necessary, logarithmic or square root transformations were used as required to improve normality. In addition, to reduce the influence of extreme values, data were converted to standard scores using the median absolute deviation method and standard scores with absolute values >2.57 or >1.96 (i.e., $P < 0.01$ or $P < 0.05$, respectively) were excluded. Effects of between-diet and within-treatment subjects factors were analyzed by mixed ANOVA followed by the Bonferroni-Holm post hoc test (30). A paired or unpaired Student *t*-test was used for separate comparisons of two groups at single time points. Areas under the curve (AUCs) were calculated using the trapezoidal rule, and analyzed by paired *t*-test. In vitro data were analyzed using nonlinear regressions with the log (agonist) versus response logistic equation for a three- or four-parameter model, respectively, to assess the best-fit values for logEC₅₀ (EC₅₀), 95% confidence interval logEC₅₀ (95% confidence interval EC₅₀), and R² (see supplementary Table VI). For each experiment, the two models were fit and standard statistical pairwise comparisons of the models and an extra sum-of-squares F test was performed. In addition,

repeated measures one-way ANOVA was performed for each single log concentration-response curve to look for an overall dose effect and simple one-way ANOVA was conducted to test differences in logEC₅₀ values between the four different log concentration-response curves. Not normally distributed data were analyzed with the Mann-Whitney U test (diet) or Wilcoxon signed-rank test (treatment, time). Data are expressed as means \pm SEM or as median. Differences are considered significant when $P < 0.05$.

RESULTS

Acute IG DGAT-1i treatment reduced energy intake in HFD-fed rats

Intragastric infusion of 3 and 9 mg/kg BW DGAT-1i reduced energy intake compared with vehicle mainly in HFD-fed rats. After 3 mg/kg BW DGAT-1i the effect was significant at 7 h (17%, $P < 0.001$) (Fig. 1A). After 9 mg/kg BW DGAT-1i (Fig. 1B) energy intake was reduced at 3, 5, 7, and 8 h (24, 18, 21, and 23% respectively; $P < 0.01$ for all) after food access. Only 9 mg/kg BW DGAT-1i reduced food intake in chow-fed rats at 7 h (14%, $P < 0.05$). There was no significant main effect of diet ($P > 0.05$, not significant) in both trials (for 2×2 mixed ANOVA test statistics see supplementary Table I). In an additional experiment without chow-fed rats, IG DGAT-1i infusion (10 mg/kg BW) reduced energy intake in 15 HFD-fed rats 1, 2, 4, 6, and 8 h after food access 22, 39, 42, 54, and 55% respectively ($P < 0.01$ for all). On the subsequent day without treatment, no difference in energy intake was observed (all time points $P > 0.05$), indicating that DGAT-1i-treated rats did not compensate for the reduction in energy intake on the following day (supplementary Fig. III).

TABLE 3. Effect of acute IG DGAT-1i infusion on circulating fat metabolites

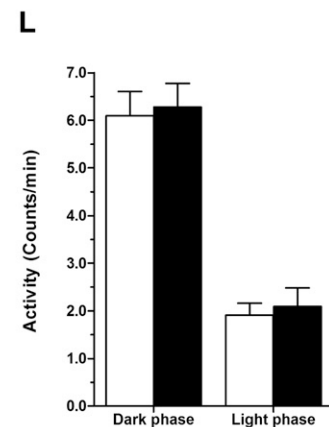
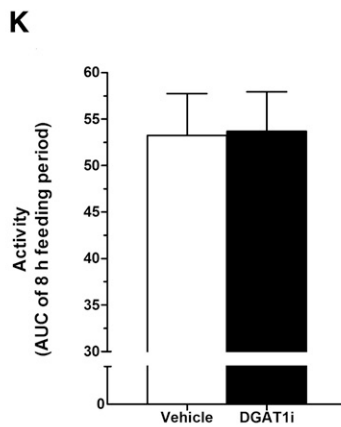
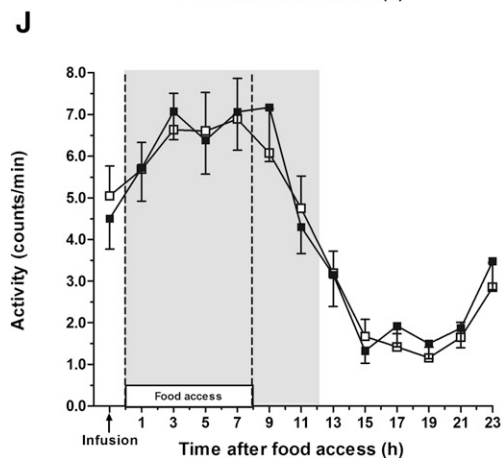
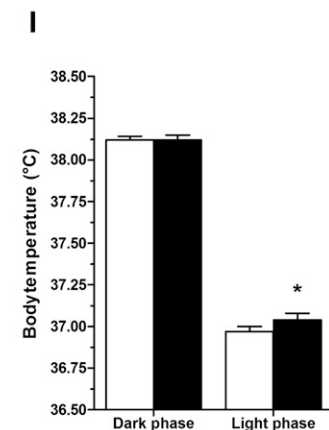
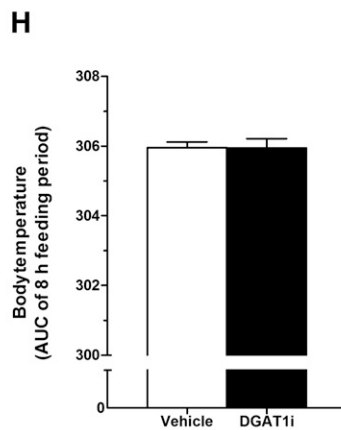
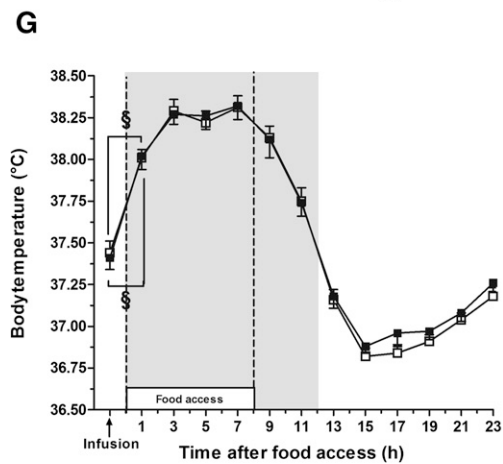
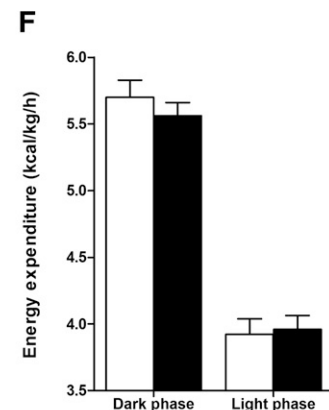
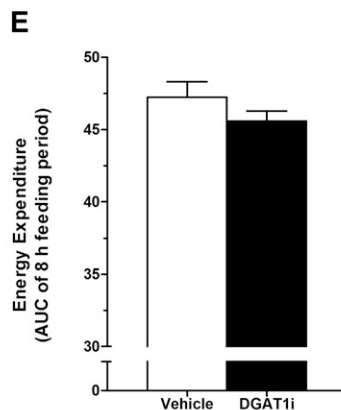
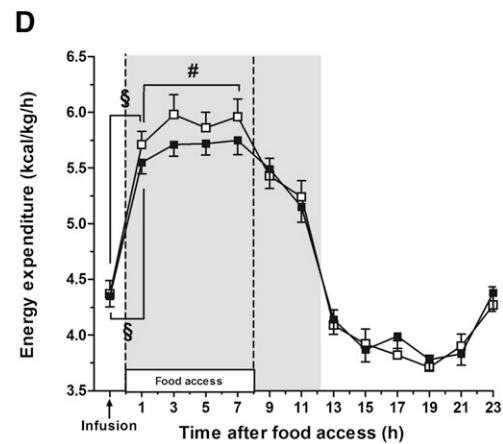
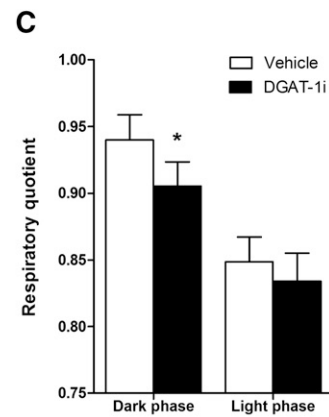
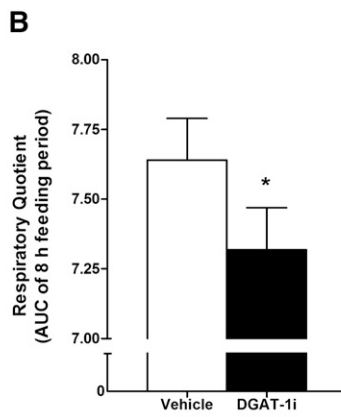
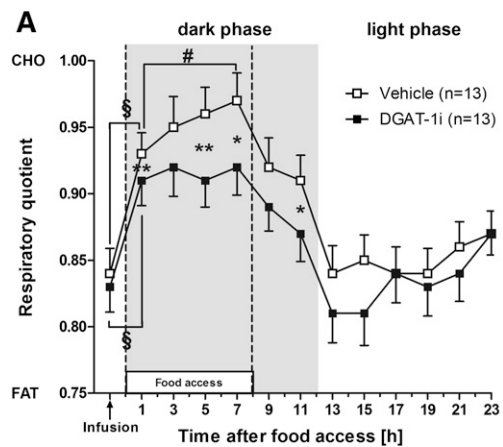
Fat Metabolites	After IG Infusion (h)	Chow		HFD	
		Vehicle	DGAT-1i	Vehicle	DGAT-1i
Serum TAG (mmol/L)	Baseline	0.20 \pm 0.04	0.19 \pm 0.04	0.27 \pm 0.03	0.25 \pm 0.06
	2 h	0.92 \pm 0.08 ^a	0.78 \pm 0.10 ^a	2.06 \pm 0.13 ^{a,b}	0.68 \pm 0.11 ^{a,c}
	3 h	1.39 \pm 0.15 ^a	1.14 \pm 0.12 ^a	2.64 \pm 0.33 ^{a,b}	0.63 \pm 0.09 ^{a,b,c}
	5 h	0.73 \pm 0.06 ^a	1.00 \pm 0.11 ^{a,c}	0.90 \pm 0.06 ^a	0.73 \pm 0.10 ^a
Plasma free glycerol (mmol/L)	Baseline	0.66 \pm 0.06	0.72 \pm 0.06	0.74 \pm 0.05	0.63 \pm 0.11
	2 h	0.08 \pm 0.02 ^a	0.06 \pm 0.02 ^a	0.18 \pm 0.01 ^{a,b}	0.11 \pm 0.03 ^{a,c}
	3 h	0.09 \pm 0.02 ^a	0.07 \pm 0.01 ^a	0.19 \pm 0.01 ^{a,b}	0.15 \pm 0.01 ^{a,b}
	5 h	0.08 \pm 0.01 ^a	0.08 \pm 0.01 ^a	0.13 \pm 0.01 ^{a,b}	0.17 \pm 0.01 ^{a,b,c}
Plasma NEFA (mmol/L)	Baseline	2.01 \pm 0.15	2.17 \pm 0.15	2.23 \pm 0.15	1.86 \pm 0.27
	2 h	0.19 \pm 0.06 ^a	0.14 \pm 0.05 ^a	0.49 \pm 0.04 ^{a,b}	0.43 \pm 0.06 ^{a,b}
	3 h	0.15 \pm 0.04 ^a	0.13 \pm 0.03 ^a	0.49 \pm 0.03 ^{a,b}	0.58 \pm 0.05 ^{a,b}
	5 h	0.29 \pm 0.04 ^a	0.24 \pm 0.02 ^a	0.36 \pm 0.04 ^a	0.60 \pm 0.04 ^{a,b,c}
Plasma BHB (μ mol/L)	Baseline	129.0 \pm 22.2	128.7 \pm 25.8	129.6 \pm 46.8	302.6 \pm 54.4 ^{b,c}
	2 h	35.6 \pm 4.3 ^a	44.1 \pm 3.5 ^a	154.6 \pm 25.5 ^b	354.7 \pm 35.4 ^{b,c}
	3 h	37.0 \pm 4.0 ^a	40.1 \pm 5.0 ^a	201.1 \pm 26.5 ^b	443.4 \pm 27.2 ^{a,b,c}
	5 h	64.6 \pm 10.8 ^a	69.3 \pm 6.0	157.3 \pm 32.8	561.0 \pm 66.1 ^{b,c}

Rats were food deprived for 16 h during light phase and refed with an isocaloric test meal consisting of 5 g chow or 3 g HFD, respectively, at dark onset. IG infusions (5 ml/kg) of DGAT-1i (9 mg/kg) or vehicle were given 1 h before dark onset. Data are presented as means \pm SEM ($n = 7$ /diet; within-subject crossover trial) and analyzed with nonparametric tests.

^a $P < 0.05$ versus baseline (Wilcoxon signed-rank test).

^b $P < 0.05$ versus chow in the same treatment group (Mann-Whitney U test).

^c $P < 0.05$ versus vehicle in the same diet group (Wilcoxon-signed rank test).



Acute IG DGAT-1i treatment caused a mild CFA

None of the flavored solutions were preferred on association days (1 h intakes for grape- and cherry-flavored solutions were 5.6 ± 0.8 ml and 6.0 ± 0.7 ml respectively; $P = 0.73$). In the two-bottle choice test rats consumed less of the flavored solutions that had been paired with IG DGAT-1i (10 mg/kg) than vehicle (32 vs. 68% preference ratio; $P < 0.001$) (Fig. 2B), indicating a mild CFA.

Acute IG DGAT-1i treatment blunted the postprandial increase in serum TAG and increased plasma BHB

Next we determined serum TAG, plasma free glycerol, NEFA, and BHB concentrations in rats treated with the DGAT-1i (9 mg/kg BW) or vehicle before and after feeding a 3 g HFD or a 5 g isocaloric chow test meal, respectively (Table 3). All rats completed the test meal within 10 min. Pretreatment baseline levels of serum TAG, plasma free glycerol, and NEFA did not differ between diets (chow vs. HFD) and treatments (vehicle vs. DGAT-1i). Baseline BHB plasma levels in HFD-fed rats were higher ($P < 0.05$) on days with DGAT-1i treatment than on days with vehicle (see below). Postprandial levels of free glycerol, NEFA, and BHB were generally higher in HFD-fed rats than in chow-fed rats irrespective of treatment, whereas only postprandial serum TAG levels of HFD-fed rats were significantly lower (45%) 3 h after DGAT-1i treatment than the corresponding values in the chow condition (all $P < 0.05$; supplementary Table II).

Furthermore, IG DGAT-1i infusion dramatically reduced the postprandial increase in serum TAG levels in HFD-fed (76%; 3 h after infusion) but not in chow-fed rats. In addition, IG DGAT-1i infusion slightly but significantly attenuated the postprandial decrease in plasma glycerol and NEFA levels in HFD- and chow-fed rats (supplementary Table III).

Finally, this marked reduction in postprandial increase of serum TAGs in DGAT-1i-treated rats was accompanied by an 85% increase in postprandial plasma BHB levels in HFD-fed rats only, indicating an increase in FAO and ketogenesis (supplementary Table IV).

Acute IG DGAT-1i treatment lowered the RQ during the feeding period without altering EE, BT or PA

To further elucidate the effect of acute pharmacological DGAT-1 inhibition on whole body FAO, we performed indirect caloric measurements in HFD-fed rats. IG DGAT-1i infusion (10 mg/kg) did not affect the increase in RQ over baseline (-1 h) observed 1 h into the feeding (and dark) period (vehicle, 11%; DGAT-1i, 10%; $P < 0.001$), but antagonized the further increase in RQ throughout the feeding period observed after vehicle (7 h vs. 1 h; vehicle, $P < 0.01$; DGAT-1i, $P = 0.24$) (Fig. 3A). As a result, compared

with vehicle, DGAT-1i reduced the RQ at 1, 5, 7, and 11 h after food access [3, 6, 5, and 4% respectively; $P < 0.01$ (1, 5 h), $P < 0.05$ (7, 11 h)] and the AUC over the 8 h feeding period ($P = 0.01$) (Fig. 3B). In addition, the RQ was lower after DGAT-1i than after vehicle treatment during the dark (feeding) phase (4%, $P < 0.05$), but did not differ between treatments during the light phase when no food was available ($P = 0.49$) (Fig. 3C).

As with the RQ, IG DGAT-1i infusion did not affect the increase in EE observed 1 h into the feeding (dark) period (vehicle, 31%; DGAT-1i, 28%; $P < 0.001$), but antagonized the further increase during the feeding period observed after vehicle (7 h vs. 1 h; vehicle, $P < 0.05$; DGAT-1i, $P = 0.20$) (Fig. 3D). The EE AUC over the 8 h feeding period tended to be lower after DGAT-1i than after vehicle, but this difference did not reach statistical significance ($P = 0.06$) (Fig. 3E). The mean EE during dark and light phase also did not differ significantly between treatments (dark phase, $P = 0.16$; light phase, $P = 0.57$) (Fig. 3F).

IG DGAT-1i infusion did not affect BT and PA over 24 h (Fig. 3G and J, respectively), during the 8 h feeding period (Fig. 3H and K, respectively), or during the dark phase (Fig. 3I and L, respectively).

Acute IG DGAT-1i treatment did not affect dietary fat absorption

We then investigated whether acute inhibition of DGAT-1 affects dietary fat absorption. IG DGAT-1i infusion did not affect feces dry weights in HFD-fed rats [DGAT-1i (10 mg/kg), 2.5 ± 0.04 g/day; vehicle, 2.5 ± 0.10 g/day; $P = 0.76$) and did not produce any overt signs of steatorrhea (data not shown). In addition, TAGs were almost undetectable in extracted fecal fat and there was no treatment difference, suggesting efficient TAG digestion was unaffected by treatment. NEFAs were generally more abundant than TAGs in the excreted feces, but again there was no difference between DGAT-1i and vehicle treatments at any time point measured (all $P > 0.05$) (Fig. 4A). Figure 4B shows a representative TLC from a vehicle and DGAT-1i treated animal with a reference depicted on the right side of the plate.

Acute IG DGAT-1i treatment induced an upregulation of jejunal Complex III of the mitochondrial respiratory chain and of mHMG-CoAS2

While elevated BHB levels and an increase of RQ clearly indicate an increase in whole body FAO in response to DGAT-1 inhibition, the data do not allow any conclusion to be drawn as to where this increase in FAO occurs. We therefore determined the expression of enzymes involved

Fig. 3. Acute IG DGAT-1i infusion lowered the RQ (A–C), i.e., enhanced fat oxidation in HFD-fed rats during dark phase but had no effect on EE (D–F), BT (G, H), or PA (I, J). RQ, EE, BT, and PA were measured during 24 h starting 1 h before until 23 h after IG DGAT-1i (10 mg/kg; $n = 13$) or vehicle ($n = 13$) infusions. IG infusions were given 1 h before food access at dark onset. Data were averaged over 2 h periods (A, D, G, I), during the 8 h feeding period (AUCs; B, E, H, K), and during the light and dark phase (C, F, I, J). Open squares (\square) and bars represent vehicle, solid squares (\blacksquare) and bars represent DGAT-1i. Shaded areas in the figures indicate dark phase. EE data are normalized for body weight. All data are shown as means \pm SEM. * $P < 0.05$; ** $P < 0.01$ versus vehicle; [§]Significantly different as indicated ([#] $P < 0.05$, [§] $P < 0.001$). Statistics are based on paired *t*-tests for each time point separately.

in lipid catabolism in liver and small intestine. IG DGAT-1i (9 mg/kg) infusion had no effect on hepatic protein expression of CPT-1 (Fig. 5A), AMPK α and p-AMPK α (Fig. 5B), mHMG-CoAS2 (Fig. 5C), and on Complex III of the mitochondrial respiratory chain (Fig. 5D), neither in chow nor in HFD-fed rats (all $P > 0.05$; supplementary Table VA). Compared with chow feeding, however, HFD feeding significantly increased hepatic protein levels of CPT-1 (DGAT-1i, +88%; vehicle, +87%; $P < 0.05$), and the p-AMPK α /AMPK α ratio (DGAT-1i, +205%; vehicle, +224%; $P < 0.05$) (supplementary Table VB). In contrast to the lack of effect on the hepatic expression of the enzymes, IG DGAT-1i infusion markedly increased protein expression of mHMG-CoAS2 (+112%; $P < 0.05$) (Fig. 6A, C) and of the Complex III of the mitochondrial respiratory chain (+340%; $P < 0.05$) (Fig. 6B, D) specifically in the jejunum of HFD- but not of chow-fed rats (supplementary Table VA). Complex III expression also appeared to be increased in the duodenum, but this difference did not reach statistical significance. These results indicate that DGAT-1 inhibition stimulated FAO and ketogenesis primarily in the jejunum. In addition, HFD feeding itself increased protein levels of mHMG-CoA synthase in the jejunum ($P < 0.05$) but not in the liver compared with chow feeding (supplementary Table VB).

DGAT-1i incubation enhanced FAO in CaCo2 and HuTu80 cells

In support of the *in vivo* findings DGAT-1i incubation triggered an increase in FAO products over a range of concentrations (0.0001–10 μM) in both CaCo2 (Fig. 7A) and HuTu80 (Fig. 7B–D) cells as assessed by the uptake of ^{14}C -palmitate (Fig. 7A, B) or ^{14}C -oleate (Fig. 7C, D) and release of ^{14}C -CO $_2$ and ^{14}C -ASP. The molar concentration of DGAT-1i that produced a half-maximal response (EC_{50}) was significantly lower in HuTu80 cells (mean $\text{EC}_{50} = 0.0076 \mu\text{M}$) than in CaCo2 cells ($\text{EC}_{50} = 0.3494 \mu\text{M}$), independent from the uptake of ^{14}C -palmitate or ^{14}C -oleate, respectively. Within the HuTu80 cells there was no significant difference of EC_{50} values. More specifically, one-way repeated measures ANOVAs of drug doses for each concentration-response curve yielded a significant effect of doses (all $P < 0.001$). Also, simple one-way ANOVAs of $\log\text{EC}_{50}$ values revealed a significant difference of $\log\text{EC}_{50}$ values ($P < 0.001$), and subsequent post hoc Bonferroni multiple comparison tests showed significant differences between $\log\text{EC}_{50}$ values of CaCo2 and HuTu80 cells (all $P < 0.01$; for best-fit values see supplementary Table VI).

DISCUSSION

We here report that inhibition of DGAT-1, one of two known DGAT enzymes that catalyzes the final step in TAG resynthesis (6, 7) with an orally bioavailable and selective small-molecule DGAT-1 inhibitor (Compound 2) (17), reduced energy intake in rats fed a HFD, but not in rats fed chow. The effect in HFD-fed animals was accompanied by a metabolic shift from TAG synthesis to FAO and ketogenesis, as indicated by a reduction in RQ and an increase in circulating

plasma BHB. The increased expression of ketogenesis enzymes in enterocytes rather than hepatocytes *in vivo* and the stimulation of FAO in enterocyte models *in vitro* are consistent with this metabolic shift and suggest it occurred primarily in enterocytes. Together with other results implicating peripheral, but not hepatic, FAO in the control of eating (18), these findings support the hypothesis that an increase in enterocyte FAO due to DGAT-1 inhibition contributes to the observed food intake reduction.

Dgat-1 $^{-/-}$ mice are resistant to HFD-induced weight gain (8) and have reduced chylomicronemia following an oral lipid challenge, suggesting a reduced rate of intestinal TAG absorption (11). Many features of dgat-1 $^{-/-}$ mice appear to be mimicked by pharmacological interference [reviewed by Birch, Buckett, and Turnbull (14)], but global gene deletion studies may fail to predict exactly the effects of pharmacological inhibition [e.g., (31)]. Likewise, we here report a hypophagic response to acute pharmacological DGAT-1 inhibition, whereas findings in dgat-1 $^{-/-}$ mice show an increase in food intake (8, 32), possibly because of developmental compensation. Furthermore, the fat content of the diet is obviously crucial for the reduction in food intake by DGAT-1 inhibition.

In addition, the effect of DGAT-1 inhibition on eating appears to be dose dependent, although the effectiveness of the two doses cannot be directly compared because they were administered in different trials. In another study, some of us observed a rapid onset inhibition of eating 2 h after oral administration of DGAT-1i (30 mg/kg BW) in 20 h-fasted HFD-adapted rats (33). Also, once daily administration of DGAT-1i (0.3, 1.0, and 3 mg/kg po) for 3 weeks reduced food intake and BW gain in DIO rats (16). Thus, the food intake reduction after DGAT-1 inhibition is not limited to our experimental design, but may differ depending on the experimental conditions. DGAT-1 inhibition produced a mild avoidance response. Whether this is related to the DGAT-1i's effect on enterocyte fat handling remains to be clarified, but it seems unlikely that this is the sole cause of its eating-inhibitory effect. While metabolic manipulations can induce a substantial taste aversion, such aversions do not necessarily reduce food intake and may in fact coexist with a stimulation of eating (34). In sum, it remains unclear whether DGAT-1i reduces food intake always by the same mechanism.

To possibly relate the metabolic effects of DGAT-1 inhibition to the food intake reduction, we determined circulating fat metabolite levels in rats adapted to chow or HFD after isocaloric HFD or chow test meals and found that DGAT-1 inhibition prevented the increase in serum TAG after the HFD meal, indicating that it antagonized intestinal TAG synthesis when a HFD was consumed. The failure of DGAT-1 inhibition to block the postprandial increase in serum TAG levels in chow-fed rats is surprising and cannot be explained based on the present results. Perhaps it is due to hepatic TAG synthesis and release that is not substantially inhibited by the DGAT-1i. In fact, Birch et al. (17) reported that the DGAT-1i used in our study inhibits intestinal and adipose tissue, but not hepatic DGAT-1. Also, DGAT-1 is highly expressed in small intestine and adipose tissue, but is less abundant in the liver (7).

The antagonism of the postprandial increase in TAG levels is in line with previous similar observations in global and intestine-specific *dgat-1^{-/-}* mice (11, 35). Also, DGAT-1 inhibition eliminated the postprandial increase in serum TAG in another study (36), which appears consistent with its prominent role in intestinal TAG synthesis (6) and suggests that the DGAT-1 inhibition under our conditions was incomplete. Perhaps the effect is more potent when DGAT-1 is highly active and, hence, TAG levels are elevated, as was the case 1 h after the onset of the HFD meal. A compensation of the DGAT-1 inhibition by other pathways (e.g., DAG-transacylase) similar to what has been proposed for *dgat-1^{-/-}* mice (11) is unlikely in response to short-term pharmacological inhibition. Finally, it is unclear whether a decrease in intestinal TAG synthesis suffices for the observed pronounced effect on circulating TAG, or whether it also requires an inhibition of hepatic TAG synthesis, as it occurs with chronic DGAT-1i treatment (15). The DGAT-1i that we employed can also antagonize adipose tissue TAG synthesis (17), but this cannot explain the effect described here because adipose tissue does not release TAG into the circulation. That fecal TAG was not elevated after DGAT-1i treatment indicates that fat malabsorption did not contribute to the decrease in circulating TAG levels and illustrates that enterocytes can still absorb dietary TAG when DGAT-1 is inhibited.

The failure of DGAT-1 inhibition to affect the postprandial decreases in plasma NEFA levels is consistent with previous findings in *dgat-1^{-/-}* mice (8) and suggests that the DGAT-1i acted primarily on intestinal TAG metabolism (17). The higher postprandial NEFA and free glycerol levels in HFD-fed rats than in chow-fed rats may reflect the escape of some NEFA and glycerol from lipoprotein lipase-mediated TAG uptake into tissues (37).

DGAT-1 inhibition appeared to increase ($P = 0.074$) postprandial BHB levels in HFD-fed rats. In an additional experiment in separate HFD-fed rats, DGAT-1i also increased (2.4-fold; $P < 0.05$) plasma BHB 5 h after infusion compared with vehicle (supplementary Fig. IV). This increase in circulating BHB was presumably secondary to a stimulation of the oxidation of dietary-derived FAs because hepatic ketogenesis that prevails during fasting, when adipose tissue-derived FAs are oxidized, is usually blocked by refeeding (38).

The decrease in RQ after DGAT-1i administration was mainly present during the first few hours of the dark phase when rats had access to food, suggesting an increase in the oxidation of dietary-derived FAs. Contrary to the observations in *dgat-1^{-/-}* mice (8), the reduction in RQ was not accompanied by an increase in EE or physical activity. In fact, DGAT-1 inhibition had no effect on EE, physical activity, and body temperature during the dark phase when activity is usually high, suggesting that there were no strange side effects accompanying the shift in oxidative metabolism. While all these data indicate an increase in whole body FAO in response to DGAT-1 inhibition, they do not identify the site where this increase occurred.

The effect of DGAT-1 inhibition on the expression of enzymes involved in lipid metabolism in the liver and the small intestine helps to answer this question. Consistent with previous studies (38–40), chronic HFD feeding caused an upregulation of key enzymes in lipid metabolism in both tissues, indicating that these enzymes adapt to the level of dietary fat. Also, DGAT-1 inhibition increased the expression of Complex III of the mitochondrial respiratory chain, which is closely related to FAO (41), and of mHMG-CoAS2, the rate-limiting enzyme in ketogenesis

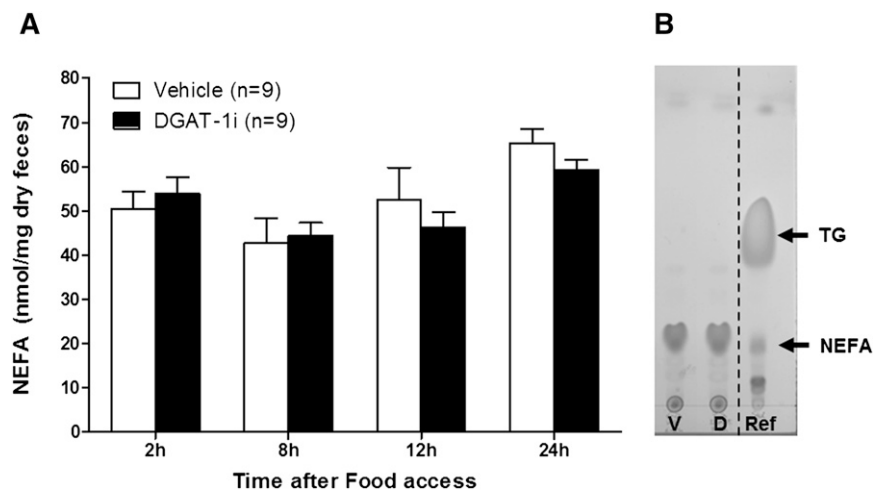


Fig. 4. Acute IG DGAT-1i infusion did not alter dietary fat absorption in HFD-fed rats as indicated by similar fecal NEFA levels. **A:** Infusions (5 ml/kg) of 10 mg/kg DGAT-1i ($n = 9$) or vehicle ($n = 9$) were given 1 h before food access at dark onset (1000 h). Feces were collected during the 8 h feeding period, 12 and 24 h after food access. Data are means \pm SEM. No treatment difference was detected at any time point (all $P > 0.05$, unpaired Student *t*-test). **B:** Sunflower oil (100 mg in 10 μ l chloroform/methanol (2:1)/mg) was used as reference (Ref). TG, triacylglycerol; V, vehicle treated rats; D, DGAT-1i treated rats.

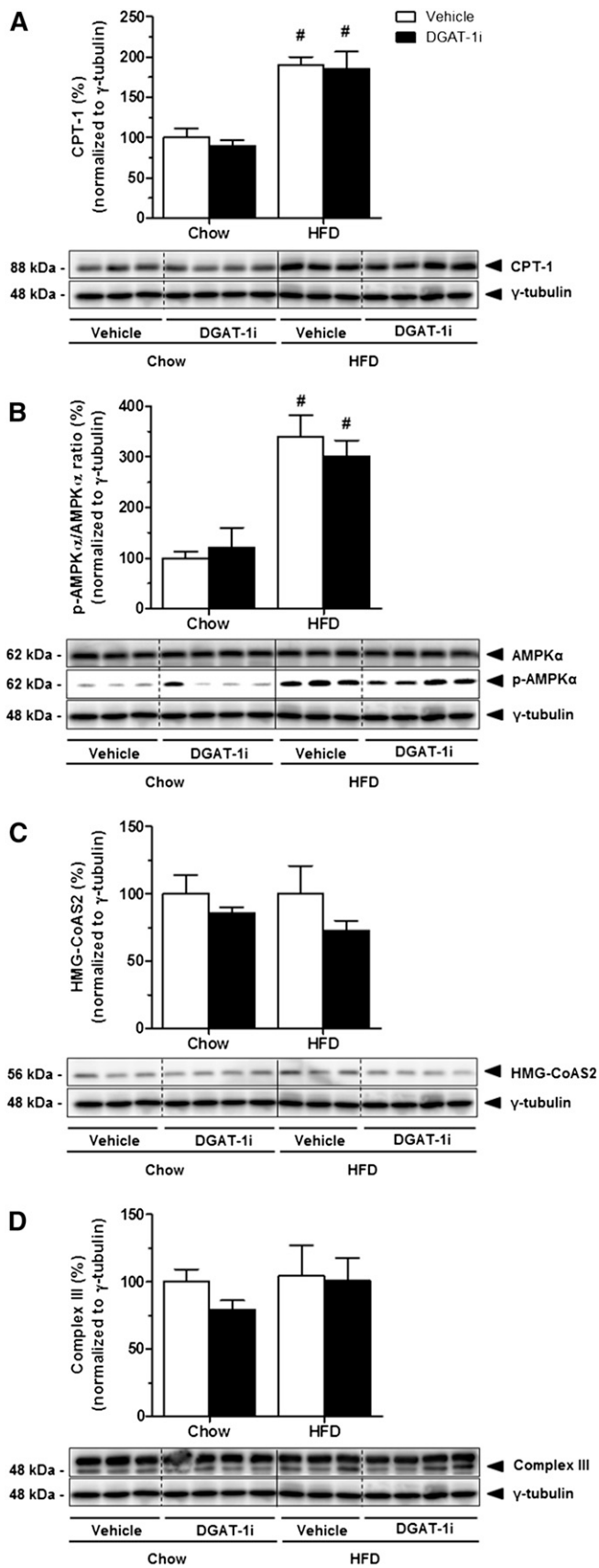


Fig. 5. Acute DGAT-1i infusion did not affect liver protein levels of CPT-1, p-AMPK α , AMPK α , HMG-CoAS2, and Complex III of the mitochondrial respiratory chain, neither in chow nor in HFD-fed rats. IG DGAT-1i (9 mg/kg) or vehicle infusions were given 1 h

(38), in the jejunum of HFD-fed rats, but not in the liver. These findings suggest that DGAT-1 inhibition under our conditions stimulated FAO and ketogenesis primarily in the jejunum. DGAT-1i infusion tended to increase expression of Complex III also in the duodenum, but this difference did not reach statistical significance. An increase in enterocyte FAO was also observed in mice lacking acyl CoA:monoacylglycerol acyltransferase-2, another enzyme involved in TAG synthesis (42). Together these findings indicate that enterocyte fat handling displays quite some plasticity with FAO and TAG synthesis apparently being reciprocally connected.

Normally, an increase in circulating NEFAs leads to an increase in circulating ketone bodies because NEFAs fuel hepatic FAO and ketogenesis. During fasting, for instance, circulating NEFAs are released from adipose tissue, and circulating ketone bodies increase because hepatic ketogenesis is enhanced. With food access, however, circulating NEFAs and ketone bodies decrease. This is mainly due to the release of insulin, which blocks lipolysis in the adipose tissue, stimulates hepatic lipogenesis, and inhibits hepatic FAO due to the inhibition of the CPT-1A, the rate-limiting enzyme of mitochondrial FAO (43). In our study, rats were food deprived for 16 h (baseline values) and had access to food at dark onset 1 h after IG DGAT-1i administration. Also, under these conditions we saw a clear decline in circulating NEFA, glycerol (inhibition of adipose tissue lipolysis), and BHB over time in chow-fed rats (see Table 3), indicating that hepatic FAO and ketogenesis were inhibited upon refeeding, as expected. In HFD-fed and DGAT-1i-treated rats, however, ketone bodies increased after refeeding. Because this increase in circulating BHB occurred in parallel to a substantial decrease in circulating NEFA, it is unlikely that it was due to an increase in hepatic ketogenesis. Further, as it occurred at a time when the expression of Complex III of the mitochondrial respiratory chain and of mitochondrial HMG-CoA synthase was increased specifically in the jejunum (and not in the liver), it is reasonable to assume that the increase in BHB production occurred in the jejunum and not in the liver. Whereas the liver is considered to be the major ketogenic organ (44), FAO and ketogenesis also occur in the small intestine during suckling. Accordingly, mHMG-CoAS2 is highly expressed in the small intestine of suckling rats (40, 45), and the small intestine regains its ketogenic capacity when pups are weaned onto, or when adult animals are adapted to a HFD (40). Thus, the capacity of the small intestine to oxidize fat (46) and to produce ketone

before food access at dark onset (1000 h). Two hours after IG infusions rats were sacrificed and liver samples were isolated. Protein extracts were prepared individually ($n = 8-9$ /diet group) and analyzed by Western blotting. Lower panels show representative Western blots for CPT-1 (A), p-AMPK α and AMPK α (B), HMG-CoAS2 (C), and Complex III (D). Upper panels show quantification of protein levels by densitometry from $n = 3-4$ rats/group. Protein levels were normalized to γ -tubulin and are presented relative to the vehicle/chow condition (100%). Values are means \pm SEM. # $P < 0.05$ versus chow within treatment group (Mann-Whitney U test).

bodies (47) increases substantially when animals are fed a HFD (40). All these findings provide indirect support for our interpretation that DGAT-1 inhibition enhances FAO and ketogenesis in the jejunum of HFD-fed animals.

How DGAT-1 inhibition stimulates intestinal mHMG-CoAS2 protein expression remains to be elucidated. Dietary DAG also stimulated FAO activity and lipid metabolism-related gene expression in the small intestine, but not in the liver, and suppressed body fat accumulation (46). The increase in intestinal FAO and ketogenesis after DGAT-1i administration in HFD-fed rats could therefore be due to a temporal increase in DAG and NEFA levels in enterocytes caused by DGAT-1 inhibition. This could help to restore normal cellular FA and DAG levels (46). A recently reported mouse model highlights the general importance of intestinal DGAT-1 inhibition (12). Expression of DGAT-1 only in the intestine completely reverses the resistance to DIO and hepatic steatosis of global *dgat-1*^{-/-}

mice, suggesting the intestine as most susceptible organ for DGAT-1 inhibition.

Supporting the *in vivo* findings, the DGAT-1i over a wide range of concentrations diverted FA away from TAG synthesis and into FAO in CaCo2 and HuTu80 cells, as assessed by measurements of the oxidation products. Given the size of the small intestine and its high expression level of DGAT-1, these findings support our hypothesis that at least some of the overall increase in FAO in response to DGAT-1i administration was due to an increase in enterocyte FAO. The lower EC₅₀ concentration of DGAT-1i in HuTu80 cells than in CaCo2 cells suggests that these cells are somehow more sensitive to DGAT-1 inhibition. Whether this has any relevance *in vivo* is uncertain.

Peripheral FAO has long been implicated in the control of eating (48), and our findings support this hypothesis because they suggest a causal relationship between the increase in FAO, in particular enterocyte FAO and ketogenesis,

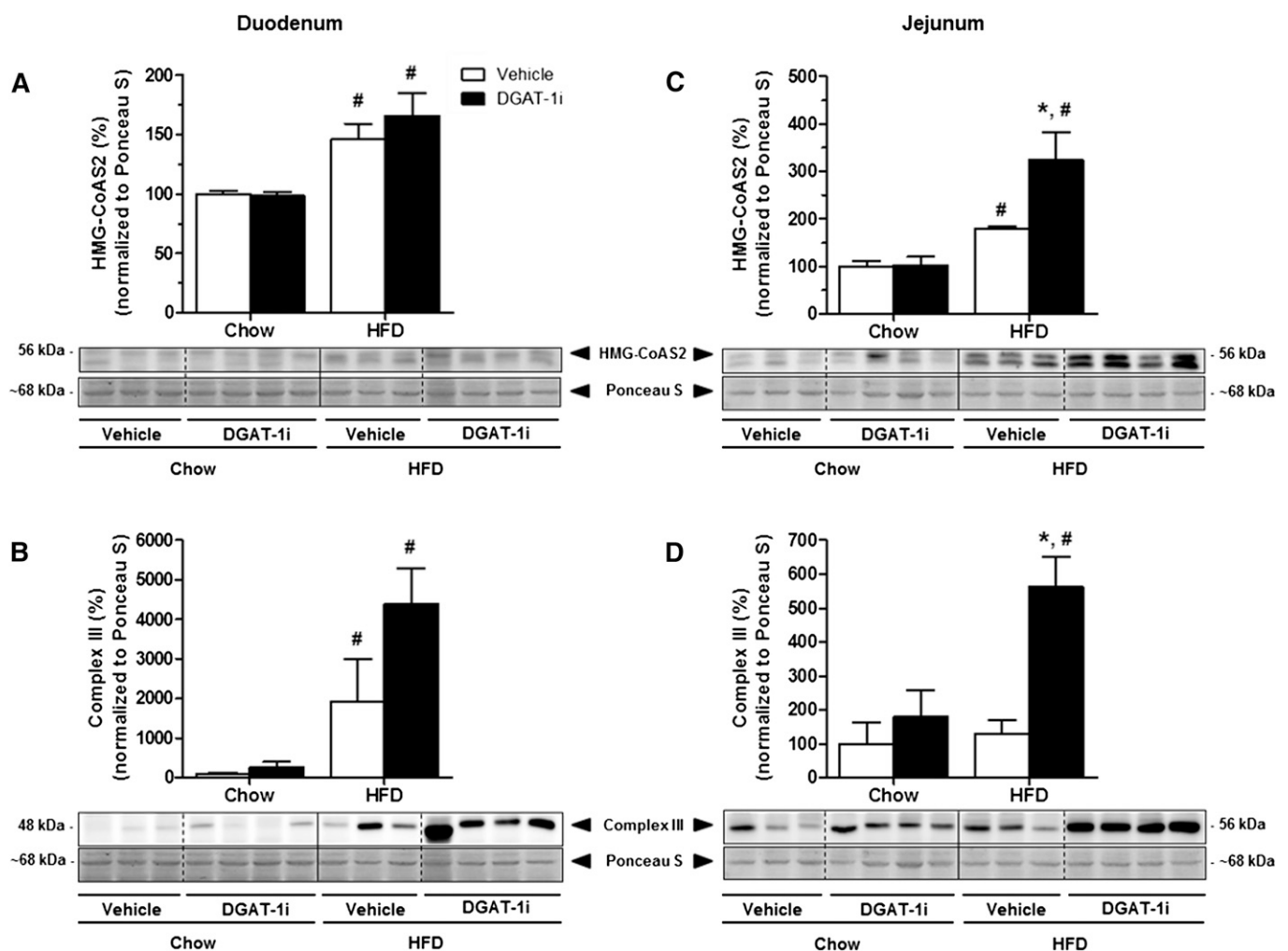


Fig. 6. Acute DGAT-1i infusion increased protein levels of HMG-CoAS2 and Complex III of the mitochondrial respiratory chain in the jejunum of HFD-fed rats but not of chow-fed rats. IG DGAT-1i (9 mg/kg) or vehicle infusions were given 1 h before food access at dark onset (1000 h). Two hours after IG infusions rats were sacrificed and small intestinal mucosa samples (duodenum and jejunum) were isolated. Protein extracts were prepared individually ($n = 8-9$ /diet group) and analyzed by Western blotting. Lower panels show representative Western blots for HMG-CoAS2 and Complex III in the duodenum (A, C) and in the jejunum (B, D) and upper panels show quantification of protein levels by densitometry from $n = 3-4$ rats/group. Protein levels were normalized to the Ponceau S signal (~ 68 kDa) and are presented relative to the vehicle/chow condition (100%). Values are means \pm SEM. * $P < 0.05$ versus vehicle within diet group; # $P < 0.05$ versus chow within treatment group (Mann-Whitney U test).

and the observed reduction of food intake after DGAT-1 inhibition. Indeed, hepatic FAO appears to be neither sufficient nor necessary for the eating-stimulatory effect of the FAO inhibitor mercaptoacetate (MA), but does require intact abdominal vagal afferents (49), suggesting that the eating-inhibitory effect of MA originates in the intestine.

The very high expression of DGAT-1 in the small intestine (7), the observation that the DGAT-1i stimulated FAO and decreased food intake only in animals fed a HFD, when postprandial FAO occurs (50) in particular in the intestine (39), the correlation and similar time courses of the inhibition of eating and the stimulation of FAO, the marked stimulation of lipid catabolism-related enzymes, and the DGAT-1i-induced increase in FAO observed in commonly used enterocyte cell culture models, all suggests a causal relationship between the increase in enterocyte FAO and the decrease in food intake after DGAT-1i administration. As mentioned above, even the increase in circulating BHB appears to be derived, at least in part, from an increase in enterocyte FAO (39, 40). A sensing

mechanism that links the energy content of dietary fat to energy intake seems plausible for several reasons (18): *i*) enterocytes themselves need substantial amounts of energy for nutrient absorption and would therefore profit from being able to generate signals that control the influx of energy into the body; and *ii*) dietary fat provides a fuel that is easily accessible through enterocyte FAO and can even be stored in the cells. Because fats are slowly absorbed through the lymphatic system, enterocytes “see” the incoming fat energy earlier than other organs and are exposed to greater meal-induced changes. Taken together, enterocytes seem to be an ideal position to quantitatively assess the incoming energy.

A possible alternative mechanism of the eating-inhibitory effect of acute DGAT-1 inhibition is a stimulation of the production and release of satiating gut peptides such as glucagon-like peptide-1 (GLP-1) and peptide tyrosine-tyrosine (PYY). GLP-1 and PYY are increased in *dgat-1*^{-/-} mice (51), and some evidence indicates that pharmacological DGAT-1 inhibition also leads to an enhanced release of these two hormones (35, 52) in addition to the

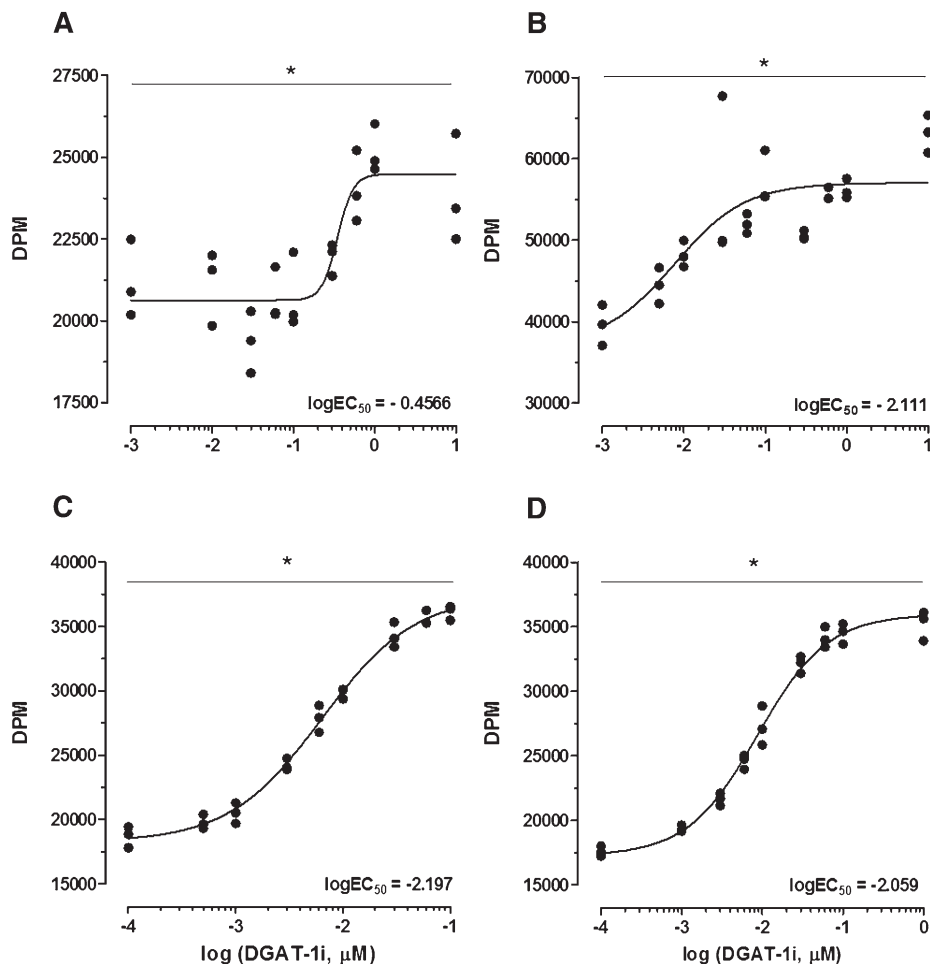



Fig. 7. DGAT-1i incubation stimulated FAO in differentiated CaCo2 (A) and HuTu80 cells (B, C, D) using 0.12 mM ¹⁴C-palmitate/BSA MR 4:1 (A, B) or 0.12 mM ¹⁴C-oleate/BSA MR 4:1 (C, D), respectively. FAO was assessed by uptake of ¹⁴C-palmitate or ¹⁴C-oleate and release of ¹⁴C-CO₂ and ¹⁴C-acid soluble products. Each data point is depicted and expressed as DPM. Individual concentration-response curves were analyzed with a one-way repeated measures ANOVA of drug doses which yielded a significant main effect of doses (**P* < 0.001; one-way repeated measure ANOVA). DPM, disintegrations per minute.

here described metabolic changes. GLP-1 and PYY inhibit eating under various circumstances (53), and may therefore also be involved in the inhibition of eating after DGAT-1 inhibition. Clearly, further studies are required to identify the exact mechanism(s) of this effect.

In summary, we show that inhibition of intestinal DGAT-1 by a small-molecular DGAT-1 inhibitor (Compound 2) (17) decreases food intake in rats and attenuates the postprandial lipidemia when the dietary fat content is high. The results indicate that DGAT-1 inhibition increases enterocyte FAO and ketogenesis when dietary fat is available, which may explain the observed whole body metabolic shift to FAO. This upregulation of intestinal lipid catabolism presumably contributes to the decrease in postprandial serum TAG levels and to the inhibition of eating. The beneficial effect of DGAT-1 inhibition on postprandial metabolism and food intake make DGAT-1 an attractive pharmacological target to counter overeating and hyperlipidemia, two hallmarks of obesity. 

The authors thank Dr. Carina Prip-Buus (INSERM U1016, CNRS UMR8104, Institut Cochin, Paris, France) for providing us with the CPT-1 antibody and Kathrin Abegg (Vetsuisse Faculty University Zurich) for help in setting up the indirect calorimetric system and analyzing metabolic measurements.

REFERENCES

- Ogden, C. L., S. Z. Yanovski, M. D. Carroll, and K. M. Flegal. 2007. The epidemiology of obesity. *Gastroenterology*. **132**: 2087–2102.
- Wilborn, C., J. Beckham, B. Campbell, T. Harvey, M. Galbreath, P. La Bounty, E. Nassar, J. Wisnann, and R. Kreider. 2005. Obesity: prevalence, theories, medical consequences, management, and research directions. *J. Int. Soc. Sports Nutr.* **2**: 4–31.
- Speakman, J. R. 2004. Obesity: the integrated roles of environment and genetics. *J. Nutr.* **134**: 2090S–2105S.
- Shi, Y., and P. Burn. 2004. Lipid metabolic enzymes: emerging drug targets for the treatment of obesity. *Nat. Rev. Drug Discov.* **3**: 695–710.
- Shi, Y., and D. Cheng. 2009. Beyond triglyceride synthesis: the dynamic functional roles of MGAT and DGAT enzymes in energy metabolism. *Am. J. Physiol. Endocrinol. Metab.* **297**: E10–E18.
- Farese, R. V., Jr., S. Cases, and S. J. Smith. 2000. Triglyceride synthesis: insights from the cloning of diacylglycerol acyltransferase. *Curr. Opin. Lipidol.* **11**: 229–234.
- Cases, S., S. J. Smith, Y. W. Zheng, H. M. Myers, S. R. Lear, E. Sande, S. Novak, C. Collins, C. B. Welch, A. J. Lusis, et al. 1998. Identification of a gene encoding an acyl CoA:diacylglycerol acyltransferase, a key enzyme in triacylglycerol synthesis. *Proc. Natl. Acad. Sci. USA.* **95**: 13018–13023.
- Smith, S. J., S. Cases, D. R. Jensen, H. C. Chen, E. Sande, B. Tow, D. A. Sanan, J. Raber, R. H. Eckel, and R. V. Farese, Jr. 2000. Obesity resistance and multiple mechanisms of triglyceride synthesis in mice lacking Dgat. *Nat. Genet.* **25**: 87–90.
- Chen, H. C., S. J. Smith, Z. Ladha, D. R. Jensen, L. D. Ferreira, L. K. Pulawa, J. G. McGuire, R. E. Pitas, R. H. Eckel, and R. V. Farese, Jr. 2002. Increased insulin and leptin sensitivity in mice lacking acyl CoA:diacylglycerol acyltransferase 1. *J. Clin. Invest.* **109**: 1049–1055.
- Chen, H. C., Z. Ladha, and R. V. Farese, Jr. 2002. Deficiency of acyl coenzyme A:diacylglycerol acyltransferase 1 increases leptin sensitivity in murine obesity models. *Endocrinology.* **143**: 2893–2898.
- Buhman, K. K., S. J. Smith, S. J. Stone, J. J. Repa, J. S. Wong, F. F. Knapp, Jr., B. J. Burri, R. L. Hamilton, N. A. Abumrad, and R. V. Farese, Jr. 2002. DGAT1 is not essential for intestinal triacylglycerol absorption or chylomicron synthesis. *J. Biol. Chem.* **277**: 25474–25479.
- Lee, B., A. M. Fast, J. Zhu, J. X. Cheng, and K. K. Buhman. 2010. Intestine-specific expression of acyl CoA:diacylglycerol acyltransferase 1 reverses resistance to diet-induced hepatic steatosis and obesity in Dgat1^{-/-} mice. *J. Lipid Res.* **51**: 1770–1780.
- King, A. J., A. S. Judd, and A. J. Souers. 2010. Inhibitors of diacylglycerol acyltransferase: a review of 2008 patents. *Expert Opin. Ther. Pat.* **20**: 19–29.
- Birch, A. M., L. K. Buckett, and A. V. Turnbull. 2010. DGAT1 inhibitors as anti-obesity and anti-diabetic agents. *Curr. Opin. Drug Discov. Devel.* **13**: 489–496.
- Zhao, G., A. J. Souers, M. Voorbach, H. D. Falls, B. Droz, S. Brodjian, Y. Y. Lau, R. R. Iyengar, J. Gao, A. S. Judd, et al. 2008. Validation of diacyl glycerol acyltransferase I as a novel target for the treatment of obesity and dyslipidemia using a potent and selective small molecule inhibitor. *J. Med. Chem.* **51**: 380–383.
- Qian, Y., S. J. Wertheimer, M. Ahmad, A. W. Cheung, F. Firooznia, M. M. Hamilton, S. Hayden, S. Li, N. Marcopulos, L. McDermott, et al. 2011. Discovery of orally active carboxylic acid derivatives of 2-phenyl-5-trifluoromethyloxazole-4-carboxamide as potent diacylglycerol acyltransferase-1 inhibitors for the potential treatment of obesity and diabetes. *J. Med. Chem.* **54**: 2433–2446.
- Birch, A. M., S. Birtles, L. K. Buckett, P. D. Kemmitt, G. J. Smith, T. J. Smith, A. V. Turnbull, and S. J. Wang. 2009. Discovery of a potent, selective, and orally efficacious pyrimidinooxazinyl bicyclooctaneacetic acid diacylglycerol acyltransferase-1 inhibitor. *J. Med. Chem.* **52**: 1558–1568.
- Langhans, W., C. Leitner, and M. Arnold. 2011. Dietary fat sensing via fatty acid oxidation in enterocytes: possible role in the control of eating. *Am. J. Physiol. Regul. Integr. Comp. Physiol.* **300**: R554–R565.
- Steffens, A. B. 1969. A method for frequent sampling of blood and continuous infusion of fluids in the rat without disturbing the animal. *Physiol. Behav.* **4**: 833–836.
- Ferrari, B., M. Arnold, R. D. Carr, W. Langhans, G. Pacini, T. B. Bodvarsdottir, and D. X. Gram. 2005. Subdiaphragmatic vagal deafferentation affects body weight gain and glucose metabolism in obese male Zucker (fa/fa) rats. *Am. J. Physiol. Regul. Integr. Comp. Physiol.* **289**: R1027–R1034.
- Baumgartner, I., G. Pacheco-Lopez, E. B. Ruttimann, M. Arnold, L. Asarian, W. Langhans, N. Geary, and J. J. Hillebrand. 2010. Hepatic-portal vein infusions of glucagon-like peptide-1 reduce meal size and increase c-Fos expression in the nucleus tractus solitarius, area postrema and central nucleus of the amygdala in rats. *J. Neuroendocrinol.* **22**: 557–563.
- Ackroff, K., and A. Sclafani. 2001. Conditioned flavor preferences: evaluating postingestive reinforcement by nutrients. Accessed March 2013, at <http://onlinelibrary.wiley.com/doi/10.1002/0471142301.ns0806fs05/abstract?sessionid=7BB886FC0EC2A8220BB752B28420B223.d02t04>.
- Labouesse, M. A., U. Stadlbauer, E. Weber, M. Arnold, W. Langhans, and G. Pacheco-Lopez. 2012. Vagal afferents mediate early satiation and prevent flavour avoidance learning in response to intraperitoneally infused exendin-4. *J. Neuroendocrinol.* **24**: 1505–1516.
- Rinaman, L., and V. Dzmura. 2007. Experimental dissociation of neural circuits underlying conditioned avoidance and hypophagic responses to lithium chloride. *Am. J. Physiol. Regul. Integr. Comp. Physiol.* **293**: R1495–R1503.
- Langhans, W. 1991. Hepatic and intestinal handling of metabolites during feeding in rats. *Physiol. Behav.* **49**: 1203–1209.
- Folch, J., M. Lees, and G. H. Sloane Stanley. 1957. A simple method for the isolation and purification of total lipides from animal tissues. *J. Biol. Chem.* **226**: 497–509.
- Riediger, T., C. Cordani, C. S. Potes, and T. A. Lutz. 2010. Involvement of nitric oxide in lipopolysaccharide induced anorexia. *Pharmacol. Biochem. Behav.* **97**: 112–120.
- Weir, J. B. 1949. New methods for calculating metabolic rate with special reference to protein metabolism. *J. Physiol.* **109**: 1–9.
- Bradford, M. M. 1976. A rapid and sensitive method for the quantitation of microgram quantities of protein utilizing the principle of protein-dye binding. *Anal. Biochem.* **72**: 248–254.
- Holm, S. 1979. A simple sequentially rejective multiple test procedure. *Scand. J. Stat.* **6**: 65–70.
- Asarian, L., B. S. Kopf, N. Geary, and W. Langhans. 2007. Pharmacological, but not genetic, disruptions in 5-HT(2C) receptor function attenuate LPS anorexia in mice. *Pharmacol. Biochem. Behav.* **86**: 493–498.
- Wang, S. J., C. Cornick, J. O'Dowd, M. A. Cawthorne, and J. R. Arch. 2007. Improved glucose tolerance in acyl CoA:diacylglycerol

- acyltransferase 1-null mice is dependent on diet. *Lipids Health Dis.* **6**: 2.
33. Birtles, S., L. K. Buckett, C. Hammon, and A. V. Turnbull. 2010. Pharmacological effect of DGAT1 inhibition on food intake and post-prandial lipaemia - determination of the mechanism of action. *Proc. Physiol. Soc.* **18**: PC28.
 34. Singer, L. K., D. A. York, H. R. Berthoud, and G. A. Bray. 1999. Conditioned taste aversion produced by inhibitors of fatty acid oxidation in rats. *Physiol. Behav.* **68**: 175–179.
 35. Ables, G. P., K. J. Yang, S. Vogel, A. Hernandez-Ono, S. Yu, J. J. Yuen, S. Birtles, L. K. Buckett, A. V. Turnbull, I. J. Goldberg, et al. 2012. Intestinal DGAT1 deficiency reduces postprandial triglyceride and retinyl ester excursions by inhibiting chylomicron secretion and delaying gastric emptying. *J. Lipid Res.* **53**: 2364–2379.
 36. King, A. J., J. A. Segreti, K. J. Larson, A. J. Souers, P. R. Kym, R. M. Reilly, C. A. Collins, M. J. Voorbach, G. Zhao, S. W. Mittelstadt, et al. 2010. In vivo efficacy of acyl CoA: diacylglycerol acyltransferase (DGAT) 1 inhibition in rodent models of postprandial hyperlipidemia. *Eur. J. Pharmacol.* **637**: 155–161.
 37. Fielding, B. 2011. Tracing the fate of dietary fatty acids: metabolic studies of postprandial lipaemia in human subjects. *Proc. Nutr. Soc.* **70**: 342–350.
 38. Hegardt, F. G. 1999. Mitochondrial 3-hydroxy-3-methylglutaryl-CoA synthase: a control enzyme in ketogenesis. *Biochem. J.* **338**: 569–582.
 39. Kondo, H., Y. Minegishi, Y. Komine, T. Mori, I. Matsumoto, K. Abe, I. Tokimitsu, T. Hase, and T. Murase. 2006. Differential regulation of intestinal lipid metabolism-related genes in obesity-resistant A/J vs. obesity-prone C57BL/6J mice. *Am. J. Physiol. Endocrinol. Metab.* **291**: E1092–E1099.
 40. Thumelin, S., M. Forestier, J. Girard, and J. P. Pegorier. 1993. Developmental changes in mitochondrial 3-hydroxy-3-methylglutaryl-CoA synthase gene expression in rat liver, intestine and kidney. *Biochem. J.* **292**: 493–496.
 41. Wang, Y., A. W. Mohsen, S. J. Mihalik, E. S. Goetzman, and J. Vockley. 2010. Evidence for physical association of mitochondrial fatty acid oxidation and oxidative phosphorylation complexes. *J. Biol. Chem.* **285**: 29834–29841.
 42. Tsuchida, T., S. Fukuda, H. Aoyama, N. Taniuchi, T. Ishihara, N. Ohashi, H. Sato, K. Wakimoto, M. Shiotani, and A. Oku. 2012. MGAT2 deficiency ameliorates high-fat diet-induced obesity and insulin resistance by inhibiting intestinal fat absorption in mice. *Lipids Health Dis.* **11**: 75.
 43. Postic, C., and J. Girard. 2008. Contribution of de novo fatty acid synthesis to hepatic steatosis and insulin resistance: lessons from genetically engineered mice. *J. Clin. Invest.* **118**: 829–838.
 44. Arias, G., G. Asins, F. G. Hegardt, and D. Serra. 1997. The effect of fasting/refeeding and insulin treatment on the expression of the regulatory genes of ketogenesis in intestine and liver of suckling rats. *Arch. Biochem. Biophys.* **340**: 287–298.
 45. Serra, D., G. Asins, and F. G. Hegardt. 1993. Ketogenic mitochondrial 3-hydroxy 3-methylglutaryl-CoA synthase gene expression in intestine and liver of suckling rats. *Arch. Biochem. Biophys.* **301**: 445–448.
 46. Murase, T., M. Aoki, T. Wakisaka, T. Hase, and I. Tokimitsu. 2002. Anti-obesity effect of dietary diacylglycerol in C57BL/6J mice: dietary diacylglycerol stimulates intestinal lipid metabolism. *J. Lipid Res.* **43**: 1312–1319.
 47. Hegardt, F. G. 1995. Regulation of mitochondrial 3-hydroxy-3-methylglutaryl-CoA synthase gene expression in liver and intestine from the rat. *Biochem. Soc. Trans.* **23**: 486–490.
 48. Scharrer, E., and W. Langhans. 1986. Control of food intake by fatty acid oxidation. *Am. J. Physiol.* **250**: R1003–R1006.
 49. Brandt, K., M. Arnold, N. Geary, W. Langhans, and M. Leonhardt. 2007. Vagal afferents mediate the feeding response to mercaptoacetate but not to the beta (3) adrenergic receptor agonist CL 316,243. *Neurosci. Lett.* **411**: 104–107.
 50. Surina, D. M., W. Langhans, R. Pauli, and C. Wenk. 1993. Meal composition affects postprandial fatty acid oxidation. *Am. J. Physiol.* **264**: R1065–R1070.
 51. Okawa, M., K. Fujii, K. Ohbuchi, M. Okumoto, K. Aragane, H. Sato, Y. Tamai, T. Seo, Y. Itoh, and R. Yoshimoto. 2009. Role of MGAT2 and DGAT1 in the release of gut peptides after triglyceride ingestion. *Biochem. Biophys. Res. Commun.* **390**: 377–381.
 52. Schober, G., M. Arnold, S. Birtles, L. K. Buckett, A. V. Turnbull, and W. Langhans. 2011. DGAT-1 inhibition increases plasma glucagon-like peptide-1 (GLP-1) and peptide tyrosine-tyrosine (PYY) levels in response to a high fat (HF) meal in rats. *Appetite.* **57**: S39.
 53. Cummings, D. E., and J. Overduin. 2007. Gastrointestinal regulation of food intake. *J. Clin. Invest.* **117**: 13–23.